Received: 17 February 2021 | Revised: 4 December 2021 | Accepted: 22 December 2021

DOI: 10.1002/nag.3322

RESEARCH ARTICLE

WILEY

One kind of transverse isotropic strength criterion and the transformation stress space

Zheng Wan[1] | **Yuanyuan Liu**[1] | **Wei Cao**[1] | **Yujia Wang**[2] | **Liyu Xie**[3] | **Yufei Fang**[4]

[1] Architectural Engineering College, North China Institute of Science and Technology, Langfang, China

[2] School of Engineering, RMIT University, Melbourne, Australia

[3] Tongji University, Shanghai, China

[4] China Academy of Railway Sciences, Beijing, China

Correspondence
Zheng Wan, Architectural Engineering College, North China Institute of Science and Technology, Langfang, 065201, China.
Email: zhengw111@126.com

Funding information
National Natural Science Foundation of China for young scholars, Grant/Award Number: 11402260; National Natural Science Foundation of China, Grant/Award Number: 42177170; Natural Science Foundation of Hebei Province in China, Grant/Award Number: E2021508031

Abstract

The geomaterials with original anisotropic properties formed in the natural process are usually simplified as a kind of cross-anisotropic material. The spatial location of the depositional plane (DP) and the effective spatial mobilized plane (ESMP) in physical space is closely related to anisotropic properties; thus, the inclined angle between DP and ESMP is taken as a primary parameter governing the strength degree of geomaterial anisotropy. According to the concept of ESMP, the frictional capacity can be more effectively mobilized when the inclined angle between DP and ESMP is larger, inducing a higher stress strength. In this study, a new stress strength formula is proposed for geomaterials, which takes the cross-anisotropic properties into account. The transformation strategy can be regarded as a strength criterion describing the convert of transversely isotropic behavior formula into an isotropic von Mises criterion formula. Based on the cross-anisotropy strength criterion, the transformed stress (TS) equation can be derived by transforming the cross-anisotropy stress space to the isotropic stress space. By using the proposed TS method, it is convenient to convert the traditional two-dimensional (2D) constitutive models on the basis of the Von-Mises criterion to the general three-dimensional (3D) models considering cross-anisotropy. Comparing the predicted and the tested results of strength and stress-strain relationship tests for geomaterials under the true triaxial loading condition, the validity and the applicability of the proposed TS method with related criterion can be ensured.

KEYWORDS
anisotropy, constitutive model, depositional plane, mobilized plane, strength

1 | INTRODUCTION

A wide variety of natural materials possess pronounced anisotropic properties, such as rock, wood, soil, and other materials, which show great differences in strengths on a macroscopic scale from various directions. Obviously, from the view of deformation and failure mechanisms, the anisotropic properties are due to the significant differences in the composition of materials at the microscopic level. Based on the test results, Oda et al.[1] confirmed that anisotropy is formed by the spatial orientation of particles and the complex interaction of soil aggregates in the process of natural deposition. For the

horizontal layered rock and soil, due to the random distribution of particles in the horizontal direction, the long axis of particles generally parallels to the horizontal depositional plane (DP), thereby forming orthotropic properties, which also known as the transversely isotropic properties.

Duncan et al.[2] found that in the undrained shear loading test, the variation in the angle between the major principal stress and the DP (when the direction of the large principal stress is different from that of the DP) yields significant difference in the results of stress-strain relationship of saturated naturally deposited clay. Abelev et al.[3,4] carried out a true triaxial drained compression test for soil samples with different inclined angles between the major principal stress and the DP. They found that the soil sample shows a higher stress strength when the direction of the major principal stress is consistent with the normal direction of the DP. However, the soil sample shows a lower stress strength when the direction of the major principal stress is perpendicular to the normal direction of the DP. Kirkgard et al.[5,6] also got the same conclusion from the test results of the clay in the San Francisco Bay area.

Yong and Silvestri[7] conducted an unconfined compression strength test on sensitive clay, the result indicates that the minimum strength value was only 60% of the maximum strength value. Nishimura et al.[8] found that the strength of naturally deposited clay was highly dependent on the direction of the deposition. Similarly, Yamada and Ishihara,[9] Ochiai and Lade,[10] Miura and Toki,[11] Hight et al,[12] Tatsuoka et al.,[13] and Pradhan et al.[14] carried out a series of triaxial compression, true triaxial loading, and hollow cylindrical torsional tests on sand, the result indicates that the strength and stress-strain relationship of naturally depositional sand are also closely related to the depositional direction. In order to describe the transversely isotropic properties, Oda et al.[15] adopted fabric tensor to describe macro statistical information such as the length and thickness ratio of microparticles shape and the distribution direction of the long axis in space. Li and Dafalias[16,17] suggested that the anisotropic properties of sand can be expressed by multiplying the stress tensor σ_{ij} with the fabric tensor F_{ij}, which can be used to establish the elastic-plastic constitutive model. Pietruszczak et al.[18] and Mroz and Maciejewski[19] proposed a strength index of cohesion and internal friction angle varying with fabric volume to reflect the effect of anisotropy on the critical limit state. To reflect the inherent anisotropy, Hashiguchi et al.[20] suggested that three principal components of the fabric tensor can be directly introduced into the rotational component of the yielding surface in the constitutive model, and the degree of anisotropy can be indicated by different initial positions of the yielding surface in the stress space.

Based on the SMP criterion, Zhang et al.[21] adopted the friction angles of the three planes that compose the SMP surface as variables that alter with the angle of the DP, and then constructed the anisotropic spatially mobilized plane (ASMP) strength criterion which can indicate the information of the DP. Cao et al.[22] introduced fabric tensor parameters into the expression of the friction law based on the SMP criterion to illustrate the anisotropic property of transversely isotropic sandy soil. Yao and Kong[23] used the inclined angle between the slip plane of SMP space and the DP as the basic variable and then constructed a stress ratio formula for the strength of transverse isotropic materials. Kong et al.[24] adopted the loading stress considering the geotechnical fabric tensor and combined it with the isotropic SMP criterion to obtain the transversely isotropic strength criterion which takes the influence of microstructure into account. Lu et al.[25] defined a strength parameter to indicate the strength of 3D transversely isotropic soil by adopting the projection of the microstructure tensor in the normal direction of the sliding surface, and then established a strength criterion for transversely isotropic soil by modifying the SMP criterion using that strength parameter. Liu,[26] Li et al.,[27] and Gao and Zhao[28,29] also combined the fabric tensors and the stresses that possess the microscopic information to investigate the anisotropic properties. In addition, Huang et al.[30] also discussed anisotropic properties from the perspective of the microscopic mechanism. Wang et al.[31] proposed the S strength criterion for the effect of the loading rate of the concrete. Considering the impact of three principal shear stresses and three normal stresses from the main shear surface of the diamond dihedral unit on the failure of materials, Gao et al.[32] proposed a unified strength criterion for the three shear stresses.

Various anisotropic criteria aforementioned above can be classified into five categories based on the following principles: (1) Modifying the existing isotropic strength criteria by considering the inclined angle between major principal stress and DP as a variable which can indicate the degree of anisotropy; (2) Improving the isotropic criteria by anisotropic state variables which can be established according to fabric tensors; (3) Revising the isotropy criterion with combined stress invariants which can be obtained by multiplying fabric tensor with the stress; (4) Based on the SMP criterion or other strength criterion, modifying the isotropic criterion by taking the inclined angle between the physical failure surface and the DP as the stress state variable; (5) Extending classical isotropic strength criterion into the anisotropic strength criterion. Each method mentioned above has its own advantages and disadvantages. It is reasonable to use the inclined angle between major principal stress and DP as the variable to evaluate the degree of anisotropy, however, the inclined angle between the major principal stress and the DP forms a "V" curve under the plane strain condition rather than a monotonic relationship. Modifying the existing strength criterion directly with the state variable of anisotropy degree expressed by

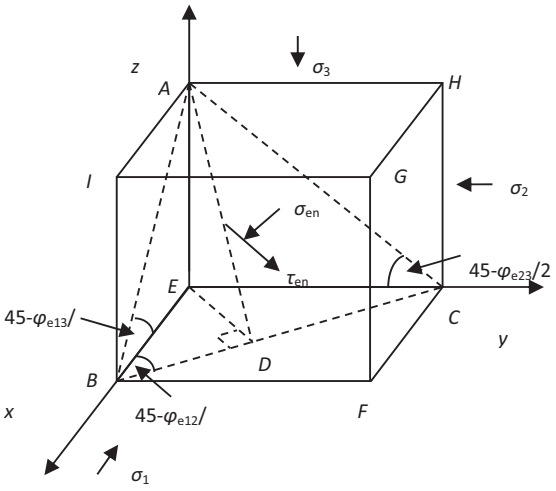

FIGURE 1 The slip plane in the three dimensional space coordinate

the fabric tensor may be practical to a certain extent, but still not universal. The method of combining fabric tensors with stress invariants can include the reasonability of anisotropy in the stresses to a certain extent, whereas the method of joint stress invariants is only at the conjecture stage without a rigorous theoretical basis. As the failure surface and the DP have clear physical meanings, and the inclined angle between them has a monotonic relationship with the anisotropic strength, the adoption of the inclined angle between the failed surface and the DP as the state variable based on a certain criterion indicates a well-normalized relationship. However, under the paths of the triaxial compression or triaxial extension tests, the failure surface needs to be screened to select the minimum strength value as more failure surfaces will occur, which may violate the material objectivity principle. The extension of the classical criterion to the anisotropic criterion only is a modification of the original criterion to a certain extent, without physical mechanism basis and the universality. Therefore, there is an urgent need for a new transformation method to consider the anisotropic strength criterion efficiently and universally.

Based on the T-strength criterion for cohesive and frictional materials proposed by Wan et al.,[33] and the physical concept of the effective slip plane, the emphasis of the current study is on the position relation of the DP. It is worth to note that the inclined angle between the effective slip plane and the material DP is used as a state variable in this study to indicate the degree of anisotropy. A large number of test results show that for many transverse isotropic materials, the angle between the loading principal stress direction and the macroscopic deposition plane or bedding plane will lead to different test failure values. For example, typical rock materials, sedimentary clay, and naturally deposited sand, other anisotropic materials also have similar properties, such as wood, bamboo and other natural materials. It can be seen that the angle between the direction of large principal stress and the direction of deposition plane or macroscopic bedding plane can be used as a state parameter affecting the final failure value. This state parameter can be chosen as one of the objective indexes to describe the influence factor to strength of transverse isotropy.

Since the T-strength criterion can transfer the von Mises criterion of metallic materials to the SMP criterion of geomaterials on the partial plane and the expression on the meridional plane is power function, it has a wide range of applications with clear physical meanings. The new anisotropic strength criterion developed based on the above anisotropic state variables can describe the anisotropic properties of different materials, such as metal, rock, concrete, clay, sand, and so on. Based on the aforementioned anisotropic strength criterion, the transformation formula is derived in the main principal stress space according to the transformation of the anisotropic T-strength criterion to the von Mises criterion proposed by Wan et al.[34] which is essentially the transformation equation from the anisotropic stress space to the isotropic stress space.

2 | *T*-STRENGTH CRITERION

Figure 1 represents the cubic element of the material and the spatially effective slip surface, that is, the ABC plane. According to the *T*-strength criterion, the material would be damaged when the stress state is on the ABC plane. According to

Figure 1, τ_{en} represents the equivalent principal shearing stress and σ_{en} denotes the main normal stress. According to the trigonometric function relation, the following relation can be deduced with the assumption of $L_{EA} = 1$.

In the right triangle ∠AEB, it can be seen that $\tan(45° - \varphi_{e13}/2) = \frac{L_{EA}}{L_{EB}}$. Based on the trigonometric function relation, the following formula can be obtained by solving the above formula:

$$L_{EB} = \tan\varphi_{e13} + \sec\varphi_{e13} \tag{1}$$

Similarly, the following relation can also be determined:

$$L_{EC} = \tan\varphi_{e23} + \sec\varphi_{e23} \tag{2}$$

where φ_{e13} represents the effective friction angle formed by the major and minor principal stresses, and φ_{e23} denotes the effective friction angle formed by the intermediate and minor principal stresses.

A parameter t has been introduced to consider the weight distribution of friction and cohesion. When $0 < t < 1$, the following relation can be obtained:

$$\tan\varphi_e = \frac{tR}{\sqrt{\sigma_0^2 - R^2}} \; 0 \le t \le 1 \tag{3}$$

Obviously, when $t = 0$, $\tan\varphi_e = 0$; when $t = 1$, $\tan\varphi_e = \frac{R}{\sqrt{\sigma_0^2 - R^2}} = \frac{(\sigma_1 - \sigma_3)}{2\sqrt{\sigma_1\sigma_3}}$.

$$\tan\varphi_{e13} = \frac{tR}{\sqrt{\sigma_0^2 - R^2}} = \frac{t(\sigma_1 - \sigma_3)}{2\sqrt{\sigma_1\sigma_3}} \tag{4}$$

$$\tan\varphi_{e23} = \frac{tR}{\sqrt{\sigma_0^2 - R^2}} = \frac{t(\sigma_2 - \sigma_3)}{2\sqrt{\sigma_2\sigma_3}} \tag{5}$$

The weight proportion of the friction force and cohesive force can be indicated by t, and the effective friction angle corresponding to the friction force and the cohesive force can be determined based on the inverse tangent of the line tangent to the outside of the Mohr circle in τ-σ space. The intercepts of the corresponding line can be expressed as:

$$L_{EB} = \frac{t(\sigma_1 - \sigma_3) + \sqrt{t^2\left(\sigma_1^2 + \sigma_3^2\right) + (4 - 2t^2)\sigma_1\sigma_3}}{2\sqrt{\sigma_1\sigma_3}} \tag{6}$$

$$L_{EC} = \frac{t(\sigma_2 - \sigma_3) + \sqrt{t^2\left(\sigma_2^2 + \sigma_3^2\right) + (4 - 2t^2)\sigma_2\sigma_3}}{2\sqrt{\sigma_2\sigma_3}} \tag{7}$$

As shown in Figure 1, since the angle ∠ABE and the angle ∠ACE are determined, the corresponding spatial slip plane can then be determined. In addition, the inclined angle between σ_1 and σ_2 is determined by the definition of the tangent value of the trigonometric function, which can be expressed as:

$$\tan\left(45° - \varphi_{e12}/2\right) = \frac{L_{EC}}{L_{EB}} \tag{8}$$

The following equation can then be derived:

$$\varphi_{e12} = 2\arctan\left(\frac{L_{EB} - L_{EC}}{L_{EB} + L_{EC}}\right) \tag{9}$$

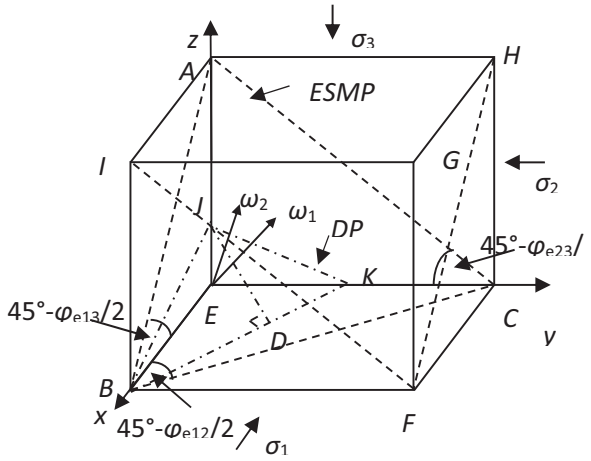

FIGURE 2 The slip plane and DP in three-dimensional space coordinates

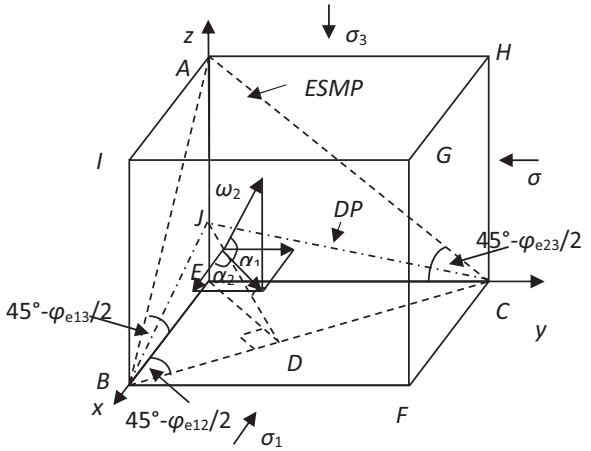

FIGURE 3 The project vector of the DP in three-dimensional space coordinates

Substituting Equations (1) and (2) into Equation (9):

$$\varphi_{e12} = 2\arctan\left(\frac{\tan\varphi_{e13} - \tan\varphi_{e23} + \sec\varphi_{e13} - \sec\varphi_{e23}}{\tan\varphi_{e13} + \tan\varphi_{e23} + \sec\varphi_{e13} + \sec\varphi_{e23}}\right) \tag{10}$$

In Equation (10), the relation of the three angles in the spatial effective slip plane used to determine the spatial position of the effective spatial mobilized plane (ESMP) has been expressed.

According to Figure 2, the ESMP of the effective slip plane can be determined after the determination of the normal direction of the plane which can be represented by the cosine.

The directional cosine of the spatial slip plane can be expressed as: $\omega_1(l_1, m_1, n_1)$. There is a spatial deposition plane (DP) of the Geotechnical materials in the spatial coordinate system, which can be represented by the direction vector of the plane. The inclined angle of the two space planes can be expressed by the arc-cosine value of the dot product of the two direction vectors if the direction cosine of the space deposition plane is expressed as $\omega_2(l_2, m_2, n_2)$. According to Figure 3. the normal line of DP can be expressed by angle α_1 and α_2.

$$\alpha = \arccos\left(\frac{l_1 l_2 + m_1 m_2 + n_1 n_2}{\sqrt{l_1^2 + m_1^2 + n_1^2}\sqrt{l_2^2 + m_2^2 + n_2^2}}\right) \tag{11}$$

The shear strength can be expressed by the stress ratio which varies with the inclined angle. When $\alpha = \alpha_{\min} = 0°$, the spatial slip plane overlaps the spatial deposition surface. Under this condition, the connection between the deposition surface is the weakest, and the shear strength is the lowest. When $\alpha = \alpha_{\max}$, the inclined angle between the spatial slip plane and the spatial deposition plane is the maximum, which represents the most difficult state for the destruction, and thus the shear strength is the highest. When $0° < \alpha < \alpha_{\max}$, the stress ratio is between the strongest and the weakest shear strength. Therefore, a relatively simple interpolation function can be determined by aforementioned two extreme stress ratios to express the anisotropic strength of materials:

$$M_\alpha = f\left(M_{\min}, M_{\max}, \alpha\right) \tag{12}$$

The normal unit vector (ω_2) of the spatial deposition plane and the projection of the normal vector in three spatial coordinate directions has been shown in Figure 3. The inclined angle between the ω_2 and xy plane equals α_1, and the inclined angle between its projection vector in the xy plane and X-axis equals α_2. The normal direction of the spatial deposition plane can then be expressed as:

$$\omega_2\left(l_2, m_2, n_2\right) = \omega_2\left(\cos\alpha_1 \cos\alpha_2,\ \cos\alpha_1 \sin\alpha_2,\ \sin\alpha_1\right) \tag{13}$$

The shear strength can be calculated as following when the angle between the effective space slip plane and the deposition plane equals 90°.

$$r = \sqrt{L_{EB}^2 + L_{EC}^2 + L_{EB}^2 L_{EC}^2} \tag{14}$$

Then, the normal vector component of the effective space slip plane can be expressed as:

$$l_1 = \frac{L_{EC}}{r} \tag{15}$$

$$m_1 = \frac{L_{EB}}{r} \tag{16}$$

$$n_1 = \frac{L_{EB} L_{EC}}{r} \tag{17}$$

$$s_{\Delta AEB} = \frac{L_{EB}}{2} \tag{18}$$

$$s_{\Delta AEC} = \frac{L_{EC}}{2} \tag{19}$$

$$s_{\Delta EBC} = \frac{L_{EB} L_{EC}}{2} \tag{20}$$

$$\sin \angle BAC = \frac{r}{\sqrt{1+r^2}} \tag{21}$$

Based on the relationship of trigonometric functions, the following relation can be obtained:

$$\tan \angle BAC = r \tag{22}$$

Based on the force balance relation of the regular tetrahedron AEBC, the equivalent normal stress can be given by:

$$\sigma_{en} = \frac{l\sigma_1 s_{\Delta AEC} + m\sigma_2 s_{\Delta AEB} + n\sigma_3 s_{\Delta EBC}}{s_{\Delta BAC}} \tag{23}$$

$$\sigma_{en} = \frac{\sigma_1 L_{EC}^2 + \sigma_2 L_{EB}^2 + \sigma_3 L_{EB}^2 L_{EC}^2}{r^2} \tag{24}$$

$$\tau_{en} = \sqrt{\left(\frac{\sigma_1 L_{EC}}{r}\right)^2 + \left(\frac{\sigma_2 L_{EB}}{r}\right)^2 + \left(\frac{\sigma_3 L_{EB} L_{EC}}{r}\right)^2 - \sigma_{en}^2} \tag{25}$$

The following formula can be obtained after derivation:

$$\tan \varphi_{mo} = \frac{L_{EB} L_{EC} \sqrt{(\sigma_1 - \sigma_2)^2 + L_{EB}^2 (\sigma_2 - \sigma_3)^2 + L_{EC}^2 (\sigma_3 - \sigma_1)^2}}{\sigma_1 L_{EC}^2 + \sigma_2 L_{EB}^2 + \sigma_3 L_{EB}^2 L_{EC}^2} \tag{26}$$

where φ_{mo} represents the internal friction angle of the space effective slip plane.

Under the triaxial compression state, Equation (26) can be expressed as:

$$\frac{\tau_{en}}{\sigma_{en}} = c_1 \tag{27}$$

The major and minor principal stresses can then be expressed as:

$$\begin{cases} \sigma_1 = p + \dfrac{2}{3} q_c \\ \sigma_2 = \sigma_3 = p - \dfrac{1}{3} q_c \end{cases} \tag{28}$$

Substituting Equation (28) into Equation (26), the function related to p and q_{c} can be obtained:

$$f(p, q_c) = \frac{q_c L_{EB_c} L_{EC_c} \sqrt{1 + L_{EC_c}^2}}{(p + 2q_c/3) L_{EC_c}^2 + (p - q_c/3) L_{EB_c}^2 \left(1 + L_{EC_c}^2\right)} \tag{29}$$

$$r_c = \sqrt{L_{EB_c}^2 + L_{EC_c}^2 + L_{EB_c}^2 L_{EC_c}^2} \tag{30}$$

Adopting the expression of the stress ratio at failure, $M = q_{\mathrm{c}}/p$, the L_{EC_c} and L_{EB_c} can be given by:

$$L_{EC_c} = 1 \tag{31}$$

$$L_{EB_c} = \frac{t q_c + \sqrt{t^2 \left(2p^2 + 5q_c^2/9 + 2pq_c/3\right) + (4 - 2t^2)\left(p^2 + pq_c/3 - 2q_c^2/9\right)}}{2\sqrt{p^2 + pq_c/3 - 2q_c^2/9}} \tag{32}$$

where M represents the failure stress ratio under the triaxial compression. If the failure stress ratio in the triaxial tension test is M_{e}, and the ratio of the triaxial tension failure stress ratio to the triaxial compression failure stress ratio is λ, then $M_{\mathrm{e}} = \lambda M$.

$$L_{EC_c} = 1 \tag{33}$$

$$r_c^2 = 2L_{EB_c}^2 + 1 \tag{34}$$

As Equation (26) and (29) are exactly equal under the path of triaxial compression, the following equation can be obtained:

$$\frac{3\sqrt{2}q_c L_{EB_c}}{(3p+2q_c)+2(3p-q_c)L_{EB_c}^2}=\frac{\sqrt{(\sigma_1-\sigma_2)^2+L_{EB}^2(\sigma_2-\sigma_3)^2+L_{EC}^2(\sigma_3-\sigma_1)^2}}{\sigma_1 L_{EC}/L_{EB}+\sigma_2 L_{EB}/L_{EC}+\sigma_3 L_{EB}L_{EC}} \tag{35}$$

Equation (35) is the formula for the shear strength of generalized deviatoric stresses in the deviatoric plane.

On the meridional plane, the hyperbolic function of the mean stress considering the hydrostatic pressure effect can be used in the expression of strength:

$$q_c = M_f p_{\mathrm{r}}\left(\frac{p+\sigma_0}{p_{\mathrm{r}}}\right)^n \tag{36}$$

2.1 | Transverse isotropic *T*-strength criterion

To consider the anisotropic property, the stress specific strength M_{f} in Equation (36) needs to be expressed as a function of the inclined angle between the effective slip surface and the deposition surface. Therefore, a relational expression for the inclined angle needs to be established with the following two requirements:

(1) The value of the strength increases with the increase in the inclined angle;
(2) The established isotropic function should satisfy the objective principle of matter where φ_{mo} at the right represents the internal friction angle of the effective slip surface. Under the anisotropic condition, $\tan\varphi_{\mathrm{mo}}$ generally is not a constant value and can be represented by the function $\tan\varphi_{\mathrm{mo}} = \mathrm{F}(\alpha, M)$. α represents the inclined angle between the slip plane and the sedimentary plane, which can be used to indicate the degree of anisotropy. Therefore, the above function involves the anisotropic direction and the degree of anisotropy.

The angle between the effective slip plane and the effective deposition plane can be expressed by the cosine as following:

$$\beta = \arccos\left[\frac{L_{EC}\cos\alpha_1\cos\alpha_2 + L_{EB}\cos\alpha_1\sin\alpha_2 + L_{EC}L_{EB}\sin\alpha_1}{r}\right] \tag{37}$$

Under the condition of triaxial compression, Equation (37) can be simplified as:

$$\beta = \arccos\left[\frac{\cos\alpha_1\cos\alpha_2 + L_{EBc}\cos\alpha_1\sin\alpha_2 + L_{EBc}\sin\alpha_1}{r_c}\right] \tag{38}$$

The joint stress invariants constructed by fabric tensor and stress invariants in accordance with certain operational rules take the contribution of the microscopic effect on shear strength into account to a certain extent. In some cases, it only considers the effect of δ between the principal stress direction and the sedimentary directions on the anisotropy strength, and monotonous relation functions between these two factors are generally established. However, the result of the plane strain test with sandy soil conducted by Matsuoka[35] shows that there is a nonmonotonic relationship between the plane strain strength and the δ, which increases first and then decreases. It has been found that the relation between the strength and the inclined angle ζ, which is between the space slip surface and the sedimentary surface, is monotonic.

Based on the regularity of the aforementioned experiments, it can be assumed that in the three-dimensional stress space, the relationship between the strength and the inclined angle which is between the slip plane and the DP is still a monotonic increasing curve. Then, the stress ratio of anisotropic strength for the inclined angle between the effective slip plane and sedimentary plane can be obtained by adopting a simple nonlinear interpolation formula:

$$M_\beta = M_n + (M_x - M_n)\left(\frac{\beta}{\beta_x}\right)^2 \tag{39}$$

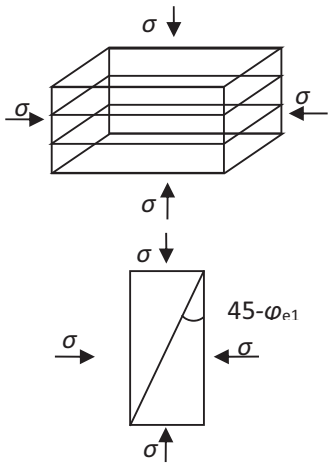

FIGURE 4 Triaxial compression condition with major principal stress perpendicular to the DP

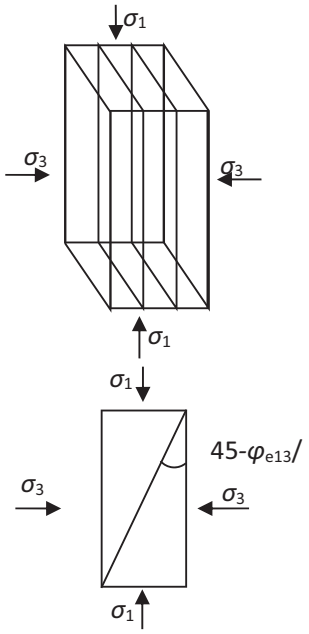

FIGURE 5 Triaxial compression condition with major principal stress parallel to the DP

where *x* stands for the abbreviation of Maximum; *n* represents the abbreviation of Minimum. It can be seen from Equation (39) that the relationship between the stress ratio of strength and the inclined angle is monotonically increasing of the quadratic function, which completely conforms to the monotonically increasing law mentioned above.

When the loading direction of the major principal stress is consistent with the normal direction of the deposition surface, the angle is the maximum which is termed as β_x. When the ESMP surface coincides with the sedimentary surface, it can be found that $\beta_n = 0$.

The *M*x can be determined by Equation (40), where φ_x is the internal friction angle determined by the triaxial compression test under the loading condition in which the deposition surface is perpendicular to the major principal stress (Figure 4). While M_n is the stress ratio of strength when $\beta = 0$, it can be determined indirectly by the stress ratio of strength M_0 obtained from the triaxial compression test on the depositional surface under the loading condition in which the major stress direction is perpendicular to the normal direction of the depositional surface (Figure 5).

$$M_x = \frac{6\sin\varphi_x}{3-\sin\varphi_x} \tag{40}$$

The minimum stress ratio of strength Mn can be obtained by the derivation of Equation (39), in which the strength value M_0 and the maximum strength value M_x obtained from conventional tests have been adopted:

$$M_n = \frac{M_0 - M_x\left[\frac{\arccos(L_{EB0}/r_0)}{\beta_x}\right]^2}{1 - \left[\frac{\arccos(L_{EB0}/r_0)}{\beta_x}\right]^2} \tag{41}$$

where

$$L_{EB0} = \frac{tM_0 + \sqrt{t^2\left(2 + 5M_0^2/9 + 2M_0/3\right) + (4 - 2t^2)\left(1 + M_0/3 - 2M_0^2/9\right)}}{2\sqrt{1 + M_0/3 - 2M_0^2/9}} \tag{42}$$

$$r_0 = \sqrt{1+2L_{EB0}^2} \tag{43}$$

$$\beta_x = \arccos\left(\frac{1}{r_x}\right) \tag{44}$$

$$r_x = \sqrt{1+2L_{EBx}^2} \tag{45}$$

$$L_{EBx} = \frac{tM_x + \sqrt{t^2\left(2 + 5M_x^2/9 + 2M_x/3\right) + (4 - 2t^2)\left(1 + M_x/3 - 2M_x^2/9\right)}}{2\sqrt{1 + M_x/3 - 2M_x^2/9}} \tag{46}$$

A primary topic considered in this research was the influence of anisotropy on triaxial compression strength. As the microscopic particles will form a certain order of the distribution under the gravity and the external effect of natural action, the long axis will parallel to the direction of deposition and the normal direction perpendicular to the sedimentary surface will be the spatial symmetry axis of the sedimentary surface when the space ellipsoid is adopted as the approximation to the cuboid particles. Since the distribution pattern in which the long axis of the particle parallel to the sedimentary surface is a stable structure for rock and soil, this pattern is very common in nature. Regarding the distribution of the spatial depositional surface, three specific cases correspond to the position of the spatial effective slip surface and the sedimentary surfaces are considered and mathematically proved by Equations (47–49):

(1) In Equation (36), if the normal direction of the sedimentary surface is consistent with the Z-axis, then $\alpha_1 = \alpha_2 = \alpha_3 = 90°$. Therefore, the inclined angle between slip surface and sedimentary surface can be given by:

$$\beta = \arccos\left[\frac{L_{EC}L_{EB}}{r}\right] \tag{47}$$

(2) If the normal direction of the sedimentary surface is consistent with the X-axis, then $\alpha_1 = \alpha_2 = 0°$, $\alpha_3 = 90°$. The inclined angle between slip surface and sedimentary surface therefore can be expressed as:

$$\beta = \arccos\left[\frac{L_{EC}}{r}\right] \tag{48}$$

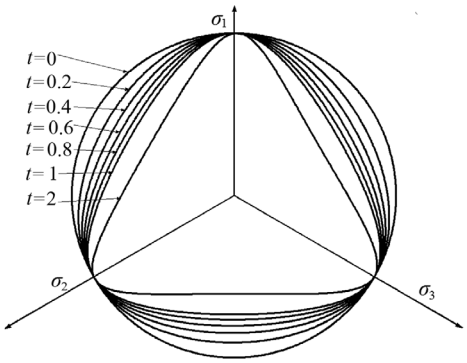

FIGURE 6 Failure surfaces with different t values at the deviatoric plane in isotropic stress space

(3) If the normal direction of the sedimentary surface is consistent with the Y-axis, then $\alpha_2 = 90°$, $\alpha_1 = \alpha_3 = 0°$. The inclined angle between slip surface and sedimentary surface can be given by:

$$\beta = \arccos\left[\frac{L_{EB}}{r}\right] \tag{49}$$

Considering the expressions of the strength in the deviatoric plane and the meridional plane, the ultimate anisotropic nonlinear strength criterion of rock and soil can be determined by simultaneously solving Equations (25), (34), (35), and (38):

$$\frac{3p\left(1+2L_{EBx}^2\right)\tan\varphi_{mo}}{3\sqrt{2}L_{EBx}-2\tan\varphi_{mo}\left(1-L_{EBx}^2\right)} - M_\beta p_r\left(\frac{p+\sigma_0}{p_r}\right)^n = 0 \tag{50}$$

Equation (50) is exactly the expression of the anisotropic strength criterion, which has been described in detail in the following.

(1) For the deviatoric plane expression of anisotropic strength criterion, Equation (50) represents the general transversely isotropic strength stress ratio when M_β not equals M_x or M_0. Under this condition, the value of the strength M_β varies with the angle of β, and the strength criterion can be regarded as the transversely isotropic T-criterion.
(2) When $M_\beta = M_x = M_0$, as the strength stress ratio of these two mutually perpendicular directions is the same, the value of strength stress ratio between these two directions is the same, the value *of* M_β becomes constant and the strength criterion degrades to the T-criterion consequently.
(3) When $t = 0$, then the strength criterion degrades to the nonlinear strength criterion which also is the SMP criterion on the deviatoric plane.
(4) When neither M_x nor M_0 is zero and $t = 0$, the strength criterion degrades to the nonlinear strength criterion which is the anisotropic SMP criterion on the deviatoric plane.

2.2 | Influence of parameters

2.2.1 | Influence of parameter t on strength criterion curve in deviatoric plane

As the essence of the strength criterion is adopting the scaling factor t as the main factor governing the shape on the deviatoric plane, the criterion is named T-criterion. Figure 6 shows that the scaling factor t, which indicates the weight of friction and cohesion, has a significant impact on the strength characteristics of materials at different stress Lode angles on the deviatoric plane. When $t = 0$, the failure of the material is only governed by the deviatoric stress strength as the effective slip angle is zero, it is therefore degraded to the generalized Mises strength criterion which represents the macroscopic failure behavior of metal materials. When $t = 1$, the T-criterion degrades to the SMP criterion which represents the failure behavior of pure frictional material. When $0 < t < 1$, it indicates the failure characteristics of materials with friction and

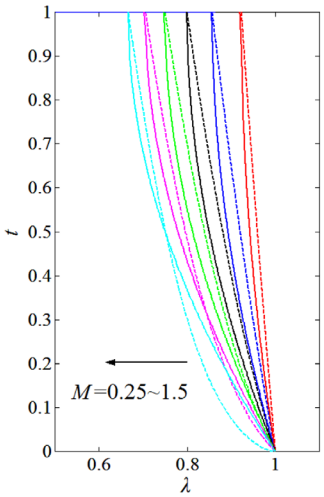

FIGURE 7 The shape functions approximated and replaced by parabolic functions

cohesion. When $t > 1$, the T-criterion represents the failure characteristics of the material that mainly governed by the stress Lode angle. According to Figure 6, the failure curve when $t = 2$ represents the tendency of the failure curve that gradually becomes the equal-triangle curve in the deviatoric plane.

As can be seen from Figure 6, the value of the deviatoric stress strength corresponding to triaxial compression is constant for different values of t. However, the values of the generalized deviatoric stress strength are different under the stress Lode angle. Therefore, the value of t can be associated with the description of the shape characteristics of the curve on the deviatoric plane. According to Figure 6, as the values of the deviatoric stress strength corresponding to triaxial extension are various, the ratio of the deviatoric stress strength of triaxial extension to the corresponding deviatoric stress strength of triaxial compression ($\lambda = q_c/q_e$) can be used as the basis for the determination of the value of t.

As Equation (35) is an implicit function of the t, the analytical expression for t cannot be obtained directly. Therefore, an explicit analytic function was considered instead of the implicit function for the determination of t. In Figure 7, the solid line represents the original implicit function, and the dotted line denotes the suggested explicit function. The detail of the explicit analytic function used to determine t can refer to the later section.

The implicit function is substituted by the proposed parabola function to determine the value of t (Figure 7). According to Figure 7, the dotted lines are used to get the exact solutions from the implicit function, and the solid lines are adopted to approximate the parabolic equation. The substitution of implicit function by the parabola function makes the calibration of the parameter t more accurate and less time-consuming. Therefore, when $\beta = 1$, then $t = 0$, which corresponds to the generalized Mises rule; when $\beta = 3/(3+M)$, then $t = 1$, which represents the SMP criterion.

Figure 8 shows the shape of the failure surface under different values of t. The spatial failure surface from inside to outside as shown in Figure 8 sequentially corresponds to five values of M_f and t ($M_f = 0.7$, 1.0, 1.4, 1.8, and 2.4; $t = 0$, 0.3, 0.6, 0.8, and 1.0). It can be seen that with the increase in the value of t, the shape of the corresponding failure surface gradually transits from the circle to the sharp curved triangle on the deviatoric plane.

Figure 9 shows the direction of major stress perpendicular to and parallel with the DP, respectively. For the isotropic T criterion, with the increase in t from 0 to 1, the strength curve on the deviatoric plane gradually transits from the curved triangle representing the SMP criterion to the circular curve which represents the von-Mises criterion. Thus, it is worth noting that t is closely related to the influence of intermediate principal stress on the strength-stress ratio, and can determine the contribution of intermediate principal stress to the strength directly.

2.2.2 | The meaning of parameter n

According to Figure 10, the failure curves from bottom to the top on the meridional plane sequentially correspond to five values of n (0.2, 0.4, 0.6, 0.8, and 1.0). The failure surface from the inside to the outside in the main stress space also corresponds to these five values of n, respectively (Figure 11). It is notable that the parameter n mainly affects the failure surface from two aspects. For the first aspect, the failure curve on the meridional plane gradually approaches

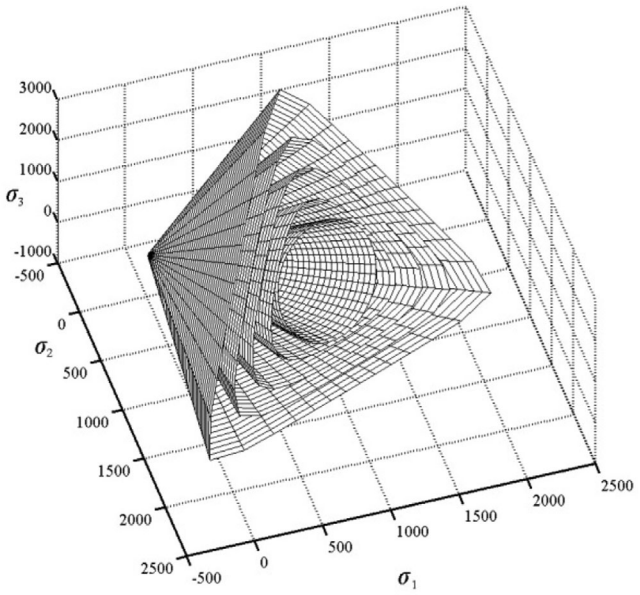

FIGURE 8 Failure surfaces in three-dimensional space with the different values of t and M_f in the principal stress space

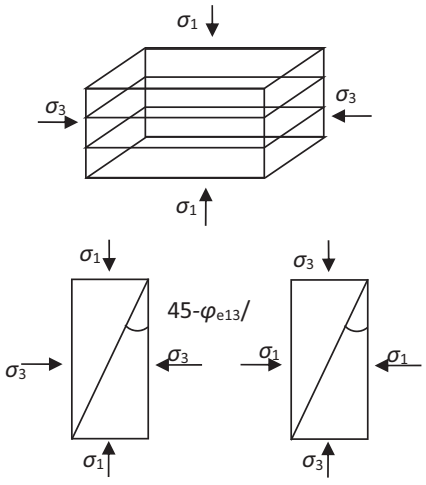

FIGURE 9 Triaxial compression and triaxial extension conditions with major principal stress perpendicular to the DP

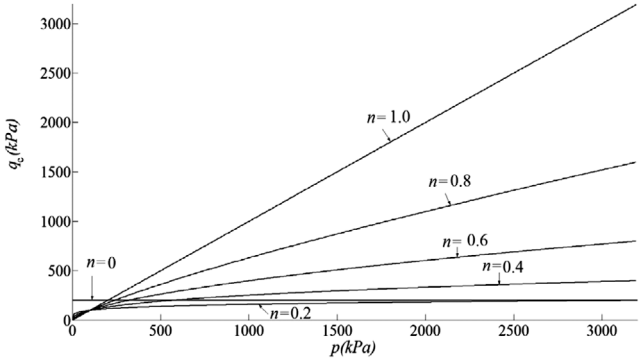

FIGURE 10 Failure curves with different values of n

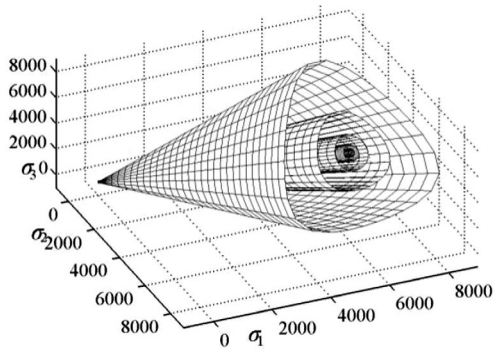

FIGURE 11 Failure surfaces in isotropic stress space with different values of n

to an oblique line with the increase in the value of n; and the failure curve gradually approaches to the horizontal line parallel to the spherical stress axis when the value of n decreases and approaches to zero. When the failure curve is a horizontal line, the generalized deviatoric stress at failure is constant, which represents that the generalized deviatoric stress plays a decisive role and is not affected by hydrostatic pressure. When the n value is between 0 and 1, the failure curve on the meridional plane corresponds to a power function curve. With the increase in the spherical stress, the generalized deviatoric stress gradually increases with a decreasing rate, which represents the nonlinear characteristics. This phenomenon indicates that the hydrostatic pressure impacts the shear strength directly under triaxial compression conditions. For the second aspect, the generalized deviatoric stress strength on the deviatoric plane under triaxial compression increases with the increase of n. Under the same spherical stress, with the increase of triaxial compression shear strength, the difference in the value of strength induced by different Lode angles gradually becomes significant, this phenomenon indicates that the degree of anisotropy gradually increases induced by the stress. Moreover, when n approaches to zero, the opening of the yield surface decreases, the deviatoric stress strength under triaxial compression and triaxial extension conditions gradually becomes equal, and the curved triangle failure surface tends to be round on the deviatoric plane, this phenomenon indicates that the isotropic property of the material is enhanced.

2.2.3 | Definition of parameter σ_0

σ_0 is the value of the left intersection of the strength curve and the hydrostatic pressure axis. The physical meaning of σ_0 is the value of the material strength under extension conditions which can indicate the cohesive properties of the material. Under the actual state, it is generally difficult to obtain the value of σ_0 under the three-direction extension, and it is set as 0 for the non-cohesion soil. For the materials with extension strength, such as the concrete, it can be set as 0.9 times the uniaxial extension strength according to Guo.[36]

2.2.4 | The meaning of parameter p_r

Parameter p_r is the characteristic pressure which can normalize shear strength q under a certain hydrostatic pressure. In addition, p_r also plays the role of making the hydrostatic pressure dimensionless; for the sand and clay, the value of p_r can be determined as the value of an atmospheric pressure. The parameter p_r can be determined according to Equation (37). The test results are arranged in a logarithmic coordinate space, and the value of p_r can then be determined according to the line fitted.

2.2.5 | Definition of parameters M_x and M_0

As the parameters used to indicate the anisotropy, the values of M_x and M_n are usually obtained by determining the triaxial compression strength under the conditions that the inclined angle between the deposition plane and the spatial effective slip plane is the maximum and the minimum. M_x can be determined by the triaxial compression strength under the loading condition in which the direction of the major principal stress is perpendicular to the deposition surface. Substituting M_0

into Equation (41), M_n can be determined indirectly, while M_0 can then be determined by the triaxial compression strength test in which the direction of major principal stress is parallel to the bedding direction of the sedimentary surface.

2.3 | Calibration of parameters

2.3.1 | Determination of parameters t

It is assumed that the tangent value of the frictional angle on the effective slip plane is the same for triaxial compression and triaxial extension. Therefore, the equation can be expressed as the following:

$$f(p, q_c) = f(p, q_e) \tag{51}$$

$$\frac{3\sqrt{2}q_c L_{EB_c}}{(3p + 2q_c) + 2(3p - q_c) L_{EB_c}^2} = \frac{\sqrt{2}q_e L_{EB_e}}{2(p + q_e/3) + (p - 2q_e/3) L_{EB_e}^2} \tag{52}$$

The ratio of the triaxial extension strength to the triaxial compression strength can be expressed as:

$$\lambda = \frac{q_e}{q_c} \tag{53}$$

$$L_{EB_c} = \frac{tq_c + \sqrt{t^2\left(2p^2 + 5q_c^2/9 + 2pq_c/3\right) + (4 - 2t^2)\left(p^2 + pq_c/3 - 2q_c^2/9\right)}}{2\sqrt{p^2 + pq_c/3 - 2q_c^2/9}} \tag{54}$$

$$L_{EB_e} = \frac{tq_e + \sqrt{t^2\left(2p^2 + 5q_e^2/9 - 2pq_e/3\right) + (4 - 2t^2)\left(p^2 - pq_e/3 - 2q_e^2/9\right)}}{2\sqrt{p^2 - pq_e/3 - 2q_e^2/9}} \tag{55}$$

Solving Equations (51–55) simultaneously, the following equation can be obtained:

$$\frac{\sqrt{2}\lambda M\left\{\dfrac{t\lambda M + \sqrt{t^2\left(2 + \frac{5}{9}\lambda^2M^2 - \frac{2}{3}\lambda M\right) + (4 - 2t^2)\left(1 - \frac{2}{9}\lambda^2M^2 - \frac{1}{3}\lambda M\right)}}{2\sqrt{1 - \frac{2}{9}\lambda^2M^2 - \frac{1}{3}\lambda M}}\right\}}{2(1 + \lambda M/3) + (1 - 2\lambda M/3)\left\{\dfrac{t\lambda M + \sqrt{t^2\left(2 + \frac{5}{9}\lambda^2M^2 - \frac{2}{3}\lambda M\right) + (4 - 2t^2)\left(1 - \frac{2}{9}\lambda^2M^2 - \frac{1}{3}\lambda M\right)}}{2\sqrt{1 - \frac{2}{9}\lambda^2M^2 - \frac{1}{3}\lambda M}}\right\}^2} = \frac{3\sqrt{2}M\left\{\dfrac{tM + \sqrt{t^2\left(2 + \frac{5}{9}M^2 + \frac{2}{3}M\right) + (4 - 2t^2)\left(1 - \frac{2}{9}M^2 + \frac{1}{3}M\right)}}{2\sqrt{1 - \frac{2}{9}M^2 + \frac{1}{3}M}}\right\}}{(3 + 2M) + 2(3 - M)\left\{\dfrac{tM + \sqrt{t^2\left(2 + \frac{5}{9}M^2 + \frac{2}{3}M\right) + (4 - 2t^2)\left(1 - \frac{2}{9}M^2 + \frac{1}{3}M\right)}}{2\sqrt{1 - \frac{2}{9}M^2 + \frac{1}{3}M}}\right\}^2} \tag{56}$$

The following formula is the recommended expression for the determination of the parameter t.

$$t = 1 - \sqrt{\lambda + \frac{3(\lambda - 1)}{M}} \tag{57}$$

2.3.2 | Determination of parameters n and Mf

The following relation can be obtained through the deformation of Equation (35):

$$\ln \frac{q_c}{p_r} = n \ln \frac{p + \sigma_0}{p_r} + \ln M_f \tag{58}$$

With the logarithms on the left and right sides of the equation, the above formula is obviously a first-order function of parameter n. Using the results of the triaxial compression test, the shear strength corresponding to different hydrostatic pressures can be arranged in the logarithmic coordinate system to fit the linear curve with slope n and intercept value $\ln M_{\mathrm{f}}$.

2.3.3 | Determination of parameters σ_0

Actually, most of soils are all granular materials without the extension strength. For rock materials with a certain extension strength, it can be determined by the extension test.

2.3.4 | Determination of parameters p_{r}

The failure line on the meridian plane is typically a nonlinear curve for geotechnical materials, which indicates that the effect of hydrostatic pressure is significant and the confining pressure would impose a considerable influence on the relationship between the deviatoric stress q and the effective mean stress p at the failure of geotechnical materials. Therefore, the curve of the relationship between q and p can be plotted over a large range of the confining pressure. The curve fitting method with a power function of p is applied and according to the minimum deviation degree of fitting, the corresponding pr value can be determined.

2.3.5 | Determination of parameters M_{x} and M_0

Since geotechnical materials in nature are of typical transversely isotropic feature, it is necessary to determine the parameters characterizing the transversely isotropy. It is clear that when the maximum principal stress direction is perpendicular to the deposition surface, the angle between the effective slip surface and the deposition surface is the maximum which corresponds to the stress ratio Mx, and also corresponds to the maximum stress ratio strength. When the angle between the effective slip surface and the deposition surface is zero, the stress ratio strength is the minimum which corresponds to the stress ratio Mn. When the maximum principal stress direction is parallel to the direction of the deposition surface, the corresponding stress ratio strength M0 is between the above values. Therefore, the value of stress ratio strength can be calculated by the internal friction angles φx and φ0 obtained from conventional triaxial compression tests with the maximum principal stress direction perpendicular to and parallel to the deposition surface.

$$M_x = \frac{6 \sin \varphi_{\mathrm{x}}}{3 - \sin \varphi_x} \tag{59}$$

$$M_0 = \frac{6 \sin \varphi_0}{3 - \sin \varphi_0} \tag{60}$$

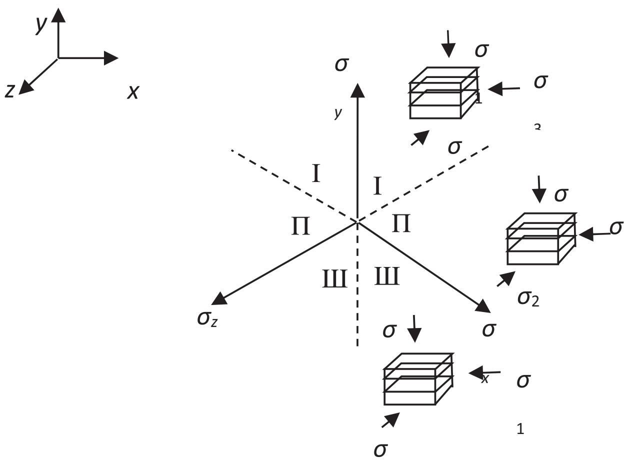

FIGURE 12 Zones describing anisotropic state in deviatoric plane

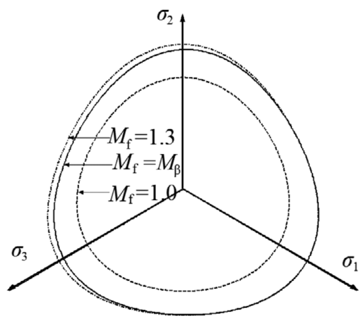

FIGURE 13 Failure surface of anisotropic criterion (DP is perpendicular to the x axis)

$$M_n = \frac{M_0 - M_x\left[\frac{\arccos(L_{EB0}/r_0)}{\beta_x}\right]^2}{1 - \left[\frac{\arccos(L_{EB0}/r_0)}{\beta_x}\right]^2} \tag{61}$$

3 | INFLUENCE OF ANISOTROPY ON STRENGTH CURVE

According to Figure 12, when the normal line of the spatial deposition plane does not coincide any axis of the three-dimensional spatial coordinate (spatial deposition plane is in a general position of the three-dimensional space), the inclined angle between the deposition plane and the effective slip plane can be expressed by Equation (37). According to Equation (39), the value of the stress specific strength is a monotonic function of the inclined angle β. The spatial location of the sedimentary surface is fixed when it has been determined. However, the effective slip surface dynamically changes with the adjustment of the principal stress value and direction. Under the non-triaxial compression condition, the value of the strength is always less than M_x. With the inclined angle alters around zero, the strength value increases or decreases correspondingly. If the inclined angle between the major principal stress and the normal direction of the deposition surface is defined as the loading angle, the value of the strength will decrease first and then increase with the loading angle.

Based on the changes of principal stress, all regions in the deviatoric plane are divided into three quadrants I, II, and III for the purpose of clear description (Figure 12).

When the normal direction of the sedimentary surface is consistent with the X-axis (σ_1 direction), it represents the isotropic strength criterion (Figure 13). When the value of M_f is constant, such as the dotted line and the dash-dotted line

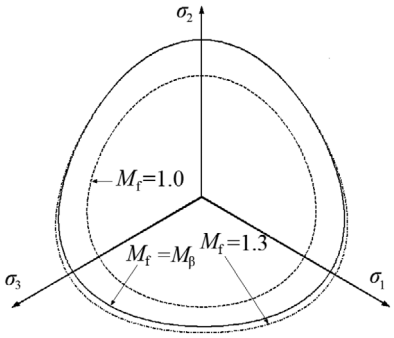

FIGURE 14 Failure surface of anisotropic criterion (DP perpendicular to the y axis)

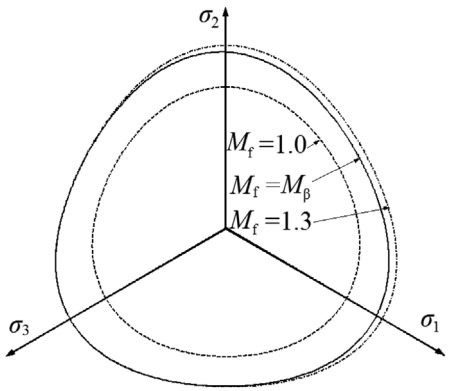

FIGURE 15 Failure surface of anisotropic criterion (DP perpendicular to the z axis)

in Figure 13, the failure curve is a symmetric graph on the deviatoric plane. When M_f is a variable, the failure curve is symmetric only with respect to the principal axis of the material.

According to Figure 14, when the sedimentary plane is perpendicular to the Y-axis, the maximum stress ratio is located on the longitudinal axis that coincides with the σ_2 axis, and the geometric failure lines on both sides are symmetrically distributed on the axis.

According to Figure 15, when the sedimentary plane is perpendicular to the Z-axis, the maximum stress ratio is located on the axis that coincides with the σ_3 axis, and the geometric failure lines on both sides are symmetrically distributed on this axis.

In general, adopting the inclined angle between the effective slip plane and the deposition plane as the state variable to indicate the degree of anisotropy can effectively demonstrate the influence of deposition plane on the strength stress ratio of the material.

4 | THE TRANSFORMATION STRESS FORMULA BASED ON THE TRANSVERSELY ISOTROPIC T-CRITERION

The two-dimensional elastoplastic model can be adopted to describe the constitutive relation influenced by the anisotropic characteristics. According to Yao et al.,[37–39] adopting the proposed transversely isotropic criterion to construct the transformation stress equation, the transversely isotropic stress space can then be transformed into an isotropic stress space. The first step is to normalize the generalized deviatoric stress q which considering the anisotropy, in other words, to convert q into q_f under a specific loading condition. In the first step, the convert of the anisotropy into isotropy is completed, and q_f is the value of the generalized deviator stress strength of triaxial compression in which the direction of the major stress is parallel with the normal direction of the deposition surface. In the second step, each component of the deviatoric stress is amplified to the point that corresponding to the von Mises circle. The third step is about to normalize the effect of principal

stress on the stress specific strength in the isotropic stress space. Through the above three steps, the transformation from anisotropic stress space to isotropic stress space can be achieved.

The shape function based on the SMP criterion proposed by Satake et al.[40] for the pure friction characteristics was on the basis of friction angle concept, therefore, the effective friction angle in this paper can replace the friction angle to obtain the shape function based on the effective friction angle:

$$q = \frac{3\sqrt{3}p\sin\varphi_{mo}}{2\sqrt{2+\sin^2\varphi_{mo}}\cos\psi} \tag{62}$$

$$\varphi_{mo} = \tan^{-1}\left[\frac{\sqrt{(\sigma_1-\sigma_2)^2 + L_{EB}^2(\sigma_2-\sigma_3)^2 + L_{EC}^2(\sigma_3-\sigma_1)^2}}{\sigma_1 L_{EC}/L_{EB} + \sigma_2 L_{EB}/L_{EC} + \sigma_3 L_{EB}L_{EC}}\right] \tag{63}$$

where L_{EB} and L_{EC} are functions of σ_1, σ_2, and σ_3, as shown in Equations (7), (8), and (26).

$$\psi = \frac{1}{3}\cos^{-1}\left[-\left(\frac{3}{2+\sin^2\varphi_{mo}}\right)^{3/2}\sin\varphi_{mo}\cos 3\theta\right] \tag{64}$$

where θ is the stress Lode angle, which can be expressed as:

$$\theta = \tan^{-1}\frac{\sqrt{3}(\sigma_2-\sigma_3)}{2\sigma_1-\sigma_2-\sigma_3} \tag{65}$$

The shape function on the deviatoric plane corresponding to the T-criterion can be expressed as:

$$g(\theta) = \frac{\sqrt{3}\left(\sqrt{8+\sin^2\varphi_{mo}} - \sin\varphi_{mo}\right)}{4\sqrt{2+\sin^2\varphi_{mo}}\cos\psi} \tag{66}$$

Since the shape function based on the T-criterion is known, the generalized deviatoric stress q_c can be obtained under the triaxial compression path corresponding to any mean stress p, which can be expressed as the following:

$$q_c = \frac{q}{g(\theta)} = \frac{6p\sin\varphi_{mo}}{\left(\sqrt{8+\sin^2\varphi_{mo}} - \sin\varphi_{mo}\right)} \tag{67}$$

Considering the correction of the anisotropy on the deviatoric plane, the T criterion with the consideration of the anisotropy on the deviatoric plane can be expressed as:

$$q_{ac} = \frac{M_f}{M_\beta}q_c = \frac{6M_f p\sin\varphi_{mo}}{M_\beta\left(\sqrt{8+\sin^2\varphi_{mo}} - \sin\varphi_{mo}\right)} \tag{68}$$

The transformation stress formula based on the anisotropic strength criterion can be expressed as the following:

$$\tilde{\sigma}_i = \begin{cases} p + \frac{q_{ac}}{q}(\sigma_i - p), & (q \neq 0) \\ \sigma_i, & (q = 0) \end{cases} \tag{69}$$

Extending it to the transformed stress formula that expressed by general stress:

$$\tilde{\sigma}_{ij} = \begin{cases} p\delta_{ij} + \frac{q_{ac}}{q}(\sigma_{ij} - p\delta_{ij}), & (q \neq 0) \\ \sigma_{ij}, & (q = 0) \end{cases} \tag{70}$$

$$\frac{\partial \tilde{\sigma}_j}{\partial \sigma_i} = \frac{1}{3} + \frac{s_j}{q}\frac{\partial q_{ac}}{\partial \sigma_i} + \frac{q_{ac}}{q}\left(\delta_{ij} - \frac{1}{3} - \frac{3}{2q^2}s_i s_j\right) \tag{71}$$

Therefore, $\frac{\partial q_{ac}}{\partial \sigma_i}$ in Equation (68) can be expressed as:

$$\frac{\partial q_{ac}}{\partial \sigma_i} = \frac{M_f}{M_\beta}\left[\frac{1}{3}\frac{\partial q_c}{\partial p} + A_5\frac{\partial q_c}{\partial \sin\varphi_{mo}}\left(1 + \tan^2\varphi_{mo}\right)^{-\frac{3}{2}}\right] \tag{72}$$

$$A_5 = B_i + \left(\frac{\partial \tan\varphi_{mo}}{\partial L_{EB}}\frac{\partial L_{EB}}{\partial \sigma_i} + \frac{\partial \tan\varphi_{mo}}{\partial L_{EC}}\frac{\partial L_{EC}}{\partial \sigma_i}\right) \tag{73}$$

$$\frac{\partial q_c}{\partial \sin\varphi_{mo}} = \frac{24p}{\left(4 + \sin^2\varphi_{mo}\right)\sqrt{8 + \sin^2\varphi_{mo}} - \sin\varphi_{mo}\left(8 + \sin^2\varphi_{mo}\right)} \tag{74}$$

Supplemented by the following:

$$\sigma_A = \left(\sigma_1 L_{EC}^2 + \sigma_2 L_{EB}^2 + \sigma_3 L_{EB}^2 L_{EC}^2\right) \tag{75}$$

$$\sigma_B = t + \frac{t^2\sigma_i + \left(2 - t^2\right)\sigma_j}{\sqrt{t^2\left(\sigma_i^2 + \sigma_j^2\right) + (4 - 2t^2)\sigma_i\sigma_j}} \tag{76}$$

$$\sigma_C = \sqrt{\frac{\sigma_j}{\sigma_i}}\left[t\left(\sigma_i - \sigma_j\right) + \sqrt{t^2\left(\sigma_i^2 + \sigma_j^2\right) + (4 - 2t^2)\sigma_i\sigma_j}\right] \tag{77}$$

$$R = \sqrt{\left(\sigma_1 - \sigma_2\right)^2 + L_{EB}^2\left(\sigma_2 - \sigma_3\right)^2 + L_{EC}^2\left(\sigma_3 - \sigma_1\right)^2} \tag{78}$$

$$\frac{\partial \tan\varphi_{mo}}{\partial L_{EB}} = \frac{1}{\sigma_A^2}\left\{\left[R \cdot L_{EC} + \frac{L_{EB}^2 \cdot L_{EC}^2\left(\sigma_2 - \sigma_3\right)^2}{R}\right]\sigma_A - 2R \cdot L_{EB}^2 \cdot L_{EC}\left(\sigma_2 + \sigma_3 L_{EC}^2\right)\right\} \tag{79}$$

$$\frac{\partial \tan\varphi_{mo}}{\partial EC} = \frac{1}{\sigma_A^2}\left\{\left[R \cdot L_{EB} + \frac{L_{EB} \cdot L_{EC}^2\left(\sigma_3 - \sigma_1\right)^2}{R}\right]\sigma_A - 2R \cdot L_{EB} \cdot L_{EC}^2\left(\sigma_1 + \sigma_3 L_{EB}^2\right)\right\} \tag{80}$$

$$\frac{\partial EB}{\partial \sigma_i} = \begin{cases} \frac{2\sqrt{\sigma_i\sigma_j}\sigma_B - \sigma_c}{4\sigma_i\sigma_j} & i \neq 2, j \neq 2 \\ 0 & i = 2 \end{cases} \tag{81}$$

TABLE 1 Geomaterial parameters

Materials	a-criterion					
	t	σ_0/MPa	p_r/MPa	M_0	n	M_x
San Francisco Bay Mud	0.33	0.0015	0.16	1.32	0.86	1.39
Cambria Sand	0.33	0.0015	0.931	1.45	0.68	1.51
Santa Monica Beach sand	0.52	0.0015	0.045	1.78	0.5	1.83
Tournemire shale	0.6	6.5	40.0	1.5	0.6	1.62
Kaolin clay	0.9	0.002	0.15	0.75	1.0	1.11
LeightonBuzzard sand	0.24	0.001	0.001	1.17	0.9	1.2
Dry pluviated sand	0.91	0.001	0.001	1.65	1.0	1.67

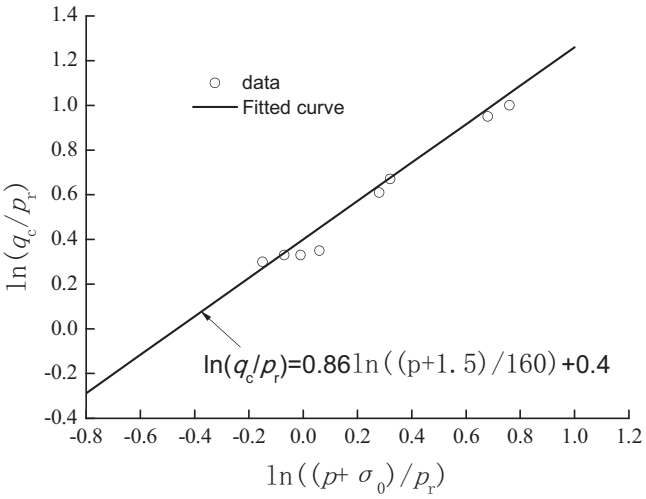

FIGURE 16 Fitted line with test data for San Francisco Bay clay

$$\frac{\partial EC}{\partial \sigma_i} = \begin{cases} 0 & i = 1 \\ \dfrac{2\sqrt{\sigma_i \sigma_j}\sigma_B - \sigma_c}{4\sigma_i \sigma_j} & i \neq 1, j \neq 1 \end{cases} \tag{82}$$

Equations (62–71) are the transformation stress formulas that convert the ordinary stress into the transformation stress space, while Equations (72–82) are the differential derivative function formulas that applying the transformation stress to the specific constitutive model in the transformation stress space.

4.1 | Criterion and test verification of stress transformation method

To facilitate the verification of the proposed transversely isotropy T-criterion and its transformation stress formula, the following geotechnical materials were used for verification analysis of failure and stress-strain relationship results under true triaxial loading test. Table 1 shows the properties of four geotechnical materials.

4.1.1 | Strength criterion prediction

The circles in Figures 16 and 17 represent the results of the conventional triaxial compression test for the San Francisco Bay clay conducted by Kirkgard and Lade. According to Figure 16, the test results were arranged in the double log coordinate

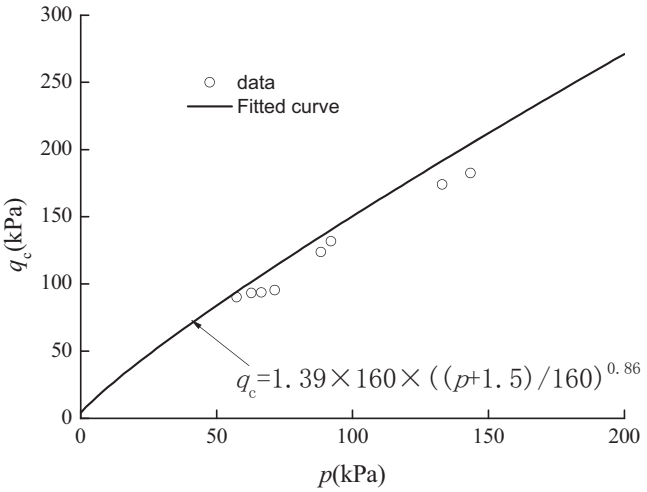

FIGURE 17 Fitted curve using power function with test data for San Francisco Bay clay

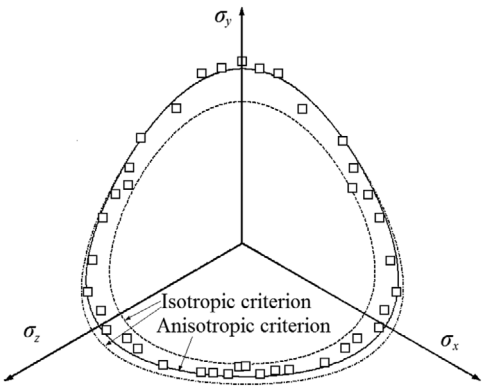

FIGURE 18 Comparison between prediction and test data for San Francisco Bay clay in deviatoric plane

system, and a straight line has been fitted as the reference curve for the calibration of the strength parameters n, p_r, and σ_0 on the meridional plane.

According to Figure 17, the test results were arranged in the p-q coordinate system. It can be seen that adopting the power function curve to fit the test results shows reasonable regularity. The parameter M_f can also be calibrated by this power function curve.

Figure 18 represents the comparison between the prediction and the test data of the failure of the San Francisco Bay clay on the deviatoric plane. The failure points are test data under the true triaxial compression condition. The dotted line and the dash-dotted line represent the failure curves predicted by isotropic T-criterion when $M_f = 1.49$ and 1.32, while the solid line represents the failure curves predicted by the proposed transversely isotropic T-criterion. The failure points present a symmetrical distribution on both sides of the Y-axis, and shows an irregular distribution pattern with the increase of stress Lode angle θ. The stress ratio strength when $\theta = 60°$ is greater than that when $\theta = 180°$. The stress-specific strength of the region corresponding to $\theta = 180°$ was overestimated by the isotropic T-criterion, while the characteristics of the strength variation in this region was better predicted by the transverse isotropic T-criterion.

Figure 19 shows the distribution law of the internal friction angle of the soil under true triaxial condition with different values of b. The circle, square lattice, and pentacle correspond to the test results from Zones I, II, and III, respectively. The solid line, dash-space line, and dash-dotted line represent the results predicted by the transverse isotropic T-criterion. Due to the failure to consider the effect of soil anisotropy, the effect of the anisotropy in different quadrants on the internal friction angle cannot be determined by the isotropic T-criterion. The dotted line in Figure 19 represents the results predicted by the isotropic T-criterion. It is notable that the difference between the results predicted by two criterions is little in the I quadrant. Based on the test results, however, the internal friction angle shows a decreasing trend in II and III quadrants, which has been indicated properly by the proposed criteria. In addition, as the effect of parameter b or the intermediate

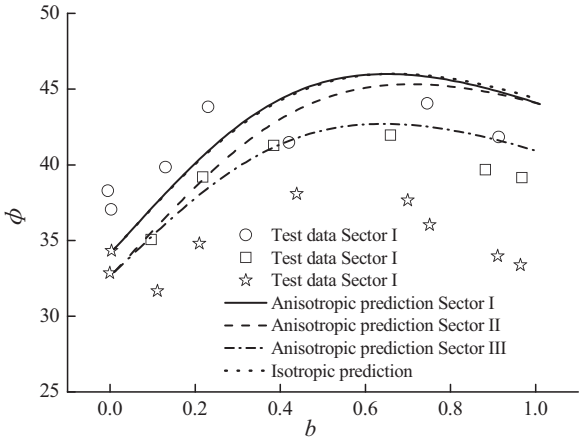

FIGURE 19 Comparison between prediction and test data of friction angle for San Francisco Bay clay with different values of *b*

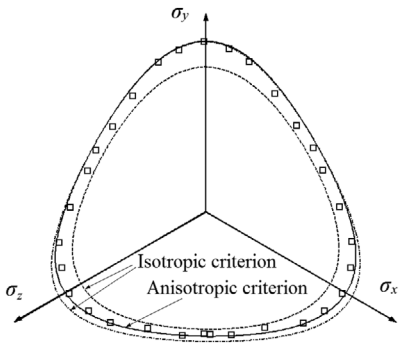

FIGURE 20 Comparison between prediction and test data for Cambria sand in deviatoric plane

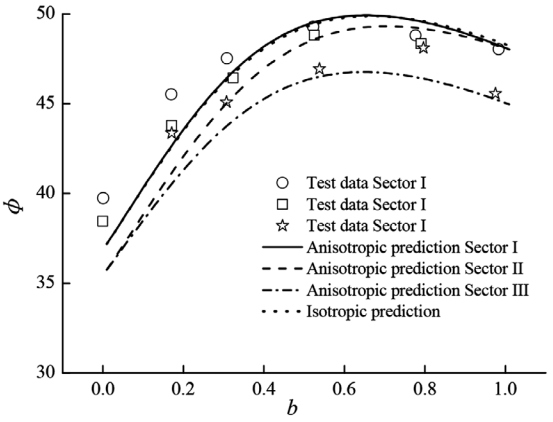

FIGURE 21 Comparison between prediction and test data of friction angle of Cambria sand with different values of *b*

principal stress on the internal friction angle can be indicated by T-criterion, the internal friction angle first increases and then decreases with the increase in the value of *b*.

The discrete points in Figure 20 are the results of true triaxial test of the Cambria sandy soil on the deviatoric plane conducted by Ochiai et al. It is worth noting that the phenomenon of low stress specific strength in the $\theta = 120°$ and 180° regions cannot be considered by the isotropic T-criterion, whereas the transverse isotropic T-criterion can reasonably overcome this limitation.

Figure 21 shows the distribution law of the internal friction angle of soil with different values of *b* under true triaxial condition. Through the comparison, it is notable that the proposed T-criterion can reasonably consider the influence of

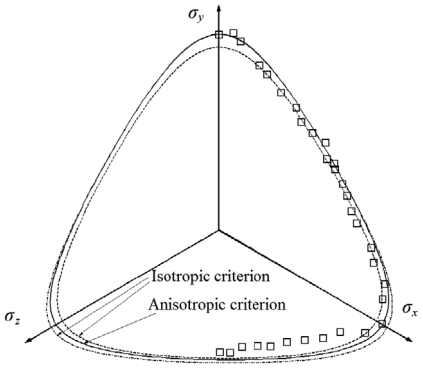

FIGURE 22 Comparison between prediction and test data for Santa Monica Beach sand in deviatoric plane

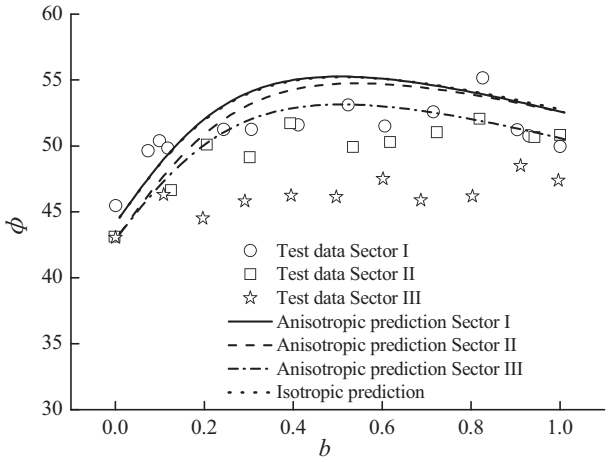

FIGURE 23 Comparison between predicted results and test data of friction angle for Santa Monica Beach sand with different b values

the principal stress coefficient b on the internal friction angle. With the increase in the value of b, the internal friction angle first increases and then decreases. The proposed T-criterion which with the consideration of the anisotropy can also indicate the overall decrease of the internal friction angle from quadrant I to III.

The discrete points in Figure 22 are the true triaxial test results of the sand on Santa Monica beach conducted by Abelev et al. Due to the discrete behavior of sand, it is more significantly affected by the middle principal stress. The projection of the cross section of the failure surface on the deviatoric plane is more similar to a sharp triangle. Due to the effect of inherent anisotropy, the deviatoric stress of $\theta = 180°$ region is smaller than that of $\theta = 60°$ region. The isotropic T-criterion overestimates the deviatoric stress strength of $\theta = 180°$ region, whereas the proposed T-criterion can indicate the lower stress specific strength of $\theta = 180°$ region accurately.

The discrete points in Figure 23 are the distribution curves of the internal friction angle affected by the values of b. Through the comparison, it is notable that the overall reduction in the internal friction angle of three quadrants can be distinguished by the transversely isotropic T-criterion clearly. When the value of b is large, the abrupt transition occurs. This phenomenon can be attributed to the effect of stress-induced anisotropy that exists in the corresponding region close to the conventional triaxial extension. However, the overall trend of the internal friction angle is still increasing first and then decreasing with the increase in the value of b.

The discrete points in Figure 24 are the conventional triaxial compression test results of the Tournemire shale under different loading angles conducted by Niandou et al.[41] The loading angle is defined as the inclined angle between the major principal stress and the normal direction of the depositional surface. It is notable that with the increase of the loading angle, the corresponding generalized deviatoric stress strength gradually decreases. On the other hand, with the increase in the average mean p stress, the generalized deviatoric stress strength increases with a significant nonlinear pattern.

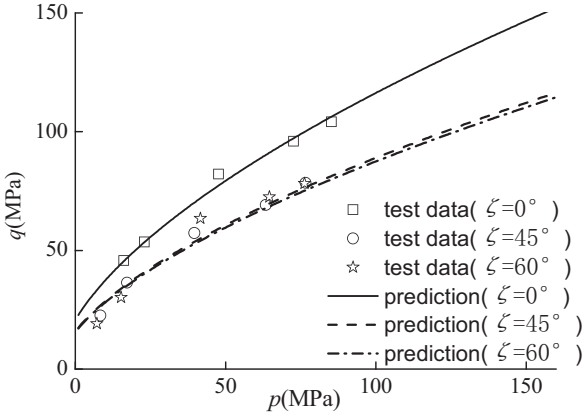

FIGURE 24 Comparison between prediction and test data of strength for Tournemire shale with different loading directions under conventional triaxial compression condition

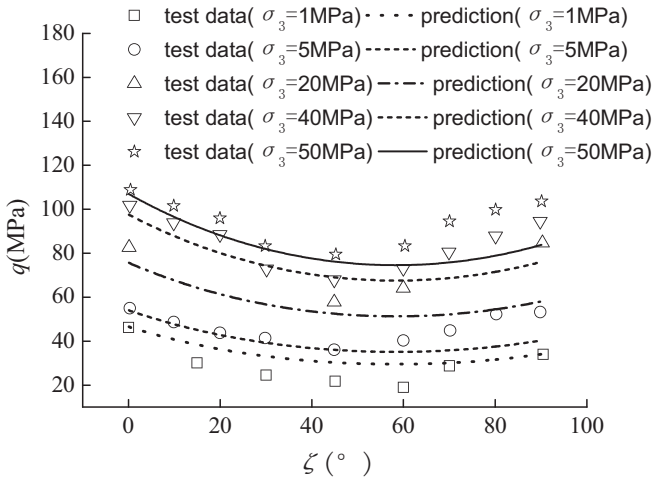

FIGURE 25 Comparison between predictions and test results on the strength of Tournemire shale with different confining pressures under conventional triaxial compression conditions

Figure 25 shows the generalized deviator stress strength of Tournemire shale with different confining pressures varies with the variation in the loading angle. With the increase in the loading angle from 0° to 90°, the value of the strength decreases first and then increases. The variation in the strength induced by the loading angle can be accurately described by the proposed transversely isotropic T-criterion. Moreover, it can be observed that the strength value when the loading angle approaches 90° is slightly lower than that of 0°, and the proposed criterion can also describe this phenomenon accurately. The predicted result of strength is slightly lower than the tested result around the 90° loading angle. This phenomenon can be attributed to two reasons: on the one hand, the influence of the microstructure of the material on macroscopic strength characteristics has not been reasonably considered; on the other hand, the predicted result is relatively high when the confining pressure is 1 MPa, which indicates that hydrostatic pressure also affects the strength of anisotropic materials. For a better prediction, the effect of the material fabric and the hydrostatic pressure should be involved in the proposed criterion.

4.2 | Application and prediction of transformation stress method

The discrete points in Figures 26–28 are the results of the conventional triaxial loading test under undrained condition conducted by Banerjee et al.[42] on kaolinite. The square represents the test result when the direction of the major principal stress is consistent with the normal direction of the depositional surface, while the round represents the test results when

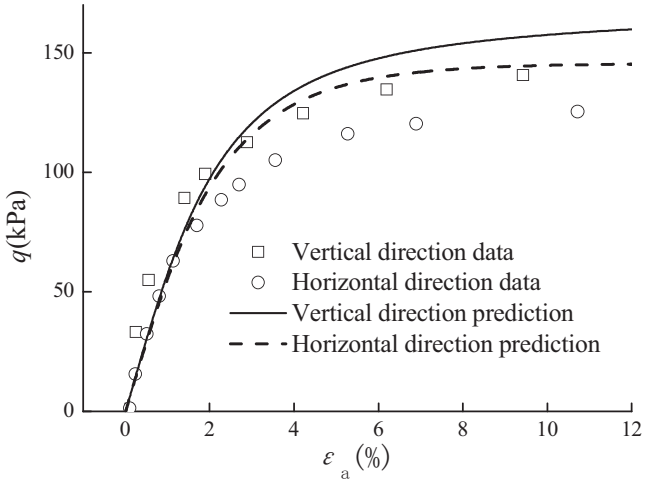

FIGURE 26 Comparison between prediction and test data of relationship between deviatoric stress and axial strain for Kaolin clay with different loading directions

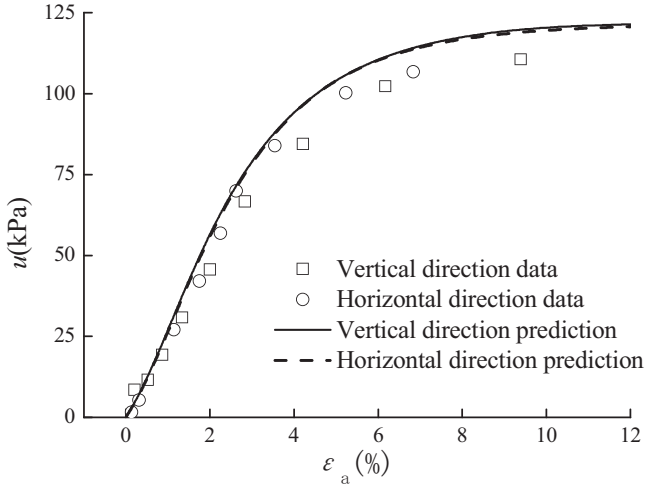

FIGURE 27 Comparison between prediction and test data of relationship between pore pressure and axial strain for Kaolin clay under different loading directions

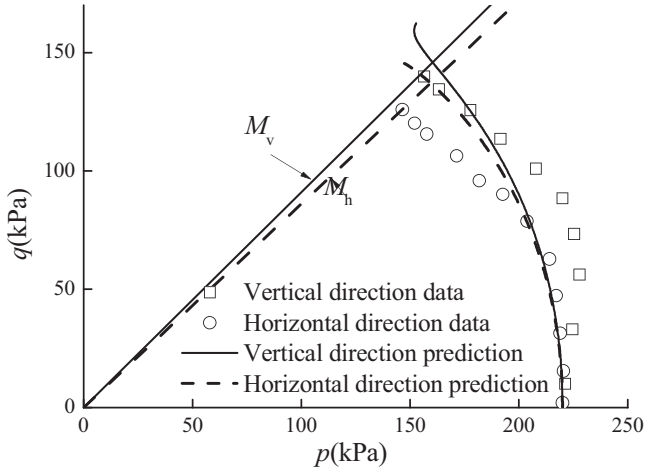

FIGURE 28 Comparison between prediction and test data of effective stress path for Kaolin clay with different loading directions

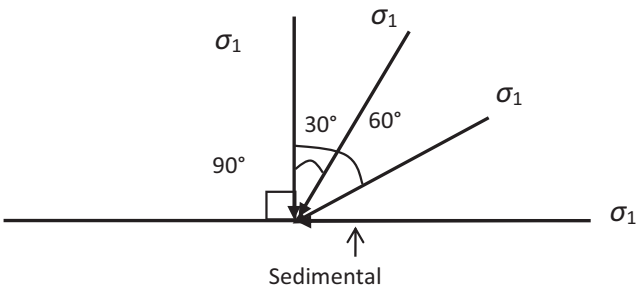

FIGURE 29 Stress paths for monotonic loading tests

the major principal stress is perpendicular to the normal direction of the sample depositional surface. The dynamic unified hardening (UH) model[43] was generalized by the proposed anisotropic transformation stress formula first, and then used this model for the following predictions. In Figures 26–28, the solid line represents the predicted results when the direction of the major principal stress is perpendicular to the sedimentary surface, while the dotted line represents the predicted result when the major principal stress is parallel to the sedimentary surface. With the consideration of the effect of transversely isotropy formed during the deposition of clay, a higher value of the elastic-plastic modulus and the shear strength yields when the maximum principal stress direction is perpendicular to the deposition surface. According to the K0 consolidation characteristics, when the loading is perpendicular to the deposition surface, the clay shows similar overconsolidation characteristics, and the initial overconsolidation stress ratio (OCR) equals 2. When the major principal stress is parallel to the deposition surface, the corresponding value of OCR is 1, which represents the characteristics of normally consolidated clay. Figures 26–28 present the influence of transverse isotropy on the stress-strain relationship under the undrained loading condition. It is notable that the loading condition with major principal stress perpendicular to the deposition surface yields a higher elastic-plastic modulus, and the effective stress path shows the characteristics of stiff clay. The difference of measured pore pressure between the two aforementioned conditions is little, and the corresponding predicted result shows a similar pattern. These results indicate the characteristics mentioned above. Figure 26 presents the relationship between the generalized deviatoric stress and the axial strain. When the direction of the major stress is perpendicular to the sedimentary phase, the tested sample yields a higher value of the modulus and the shear strength. When the directions are consistent, the tested sample yields a lower value of the modulus and the shear strength. The simulation result from the dynamic UH model generalized by the proposed anisotropic transformation stress formula indicates that the increase in the modulus and strength is completely consistent with the tested results.

Figure 27 presents the predicted results of the relation curve between the pore pressure and the major principal strain. The difference in the pore pressure between the vertical loading and parallel loading tests to the sedimentary surface is little, which indicates that the pore pressure is basically independent on the loading direction. The difference in predicted outcomes is also little.

Figure 28 presents the comparison between the tested and the predicted effective stress path. It is notable that the specimen is harder and the ultimate undrained strength is larger when the loading direction is perpendicular to the depositional surface. When the loading direction is parallel to the depositional surface, the sample is soft and the final undrained strength is lower. The predicted curve indicates this pattern.

In Figure 28, the generalized deviatoric stress strength indicates that the major principal stress is not only perpendicular to the sedimentary plane, but also larger than the major principal stress which parallel to the sedimentary plane. However, the difference of deviatoric stress between the two loading conditions is smaller than the tested results, and the tested result indicates that new difference occurs at the beginning of loading. The difference increases with the increase in the axial strain, and the difference becomes obvious when the axial strain reaches a certain value. The tested and predicted result of the relationship between pore pressure and axial strain in Figure 28 indicates this phenomenon. The effective stress path in Figure 29 shows a similar pattern. The main reason can be attributed to that the effect of anisotropy on soil deformation is not considered adequately when the model is converted into the three-dimensional stress model by modifying the strength value. The next step is to introduce the state variables that can consider the effect of anisotropy on the dilatancy law proposed by Rowe, P.[44] to fully simulate the differences in the above stress-strain relations.

Figure 29 is a schematic diagram of four loading paths with normal angles which between the major principal stress and the sedimentary plane equal 0°, 30°, 60°, and 90°, respectively. The discrete points in Figures 29–36 are the test results of the stress-strain relationship of Leighton Buzzard sand under the influence of the original anisotropy and the stress

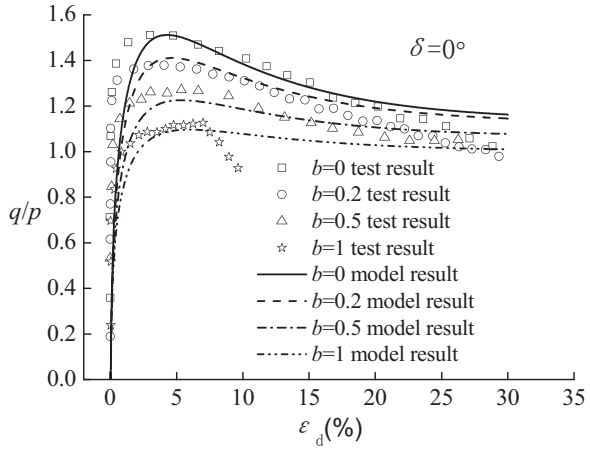

FIGURE 30 Comparison between test data and prediction of relationship between stress ratio and deviatoric strain for Leighton Buzzard sand under $\delta = 0°$

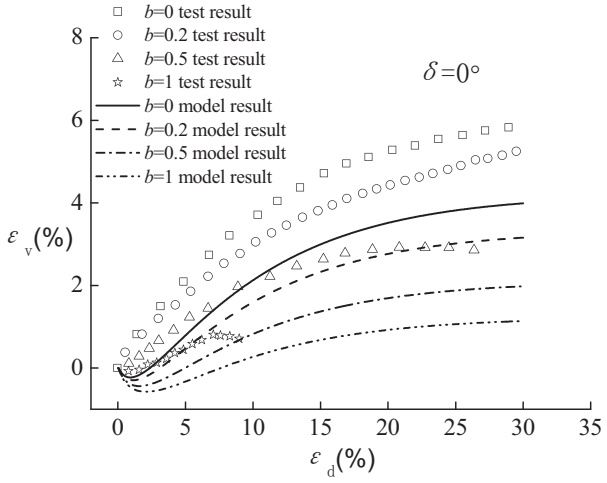

FIGURE 31 Comparison between test data and prediction of volume strain and deviatoric strain relationship for Leighton Buzzard sand under $\delta = 0°$

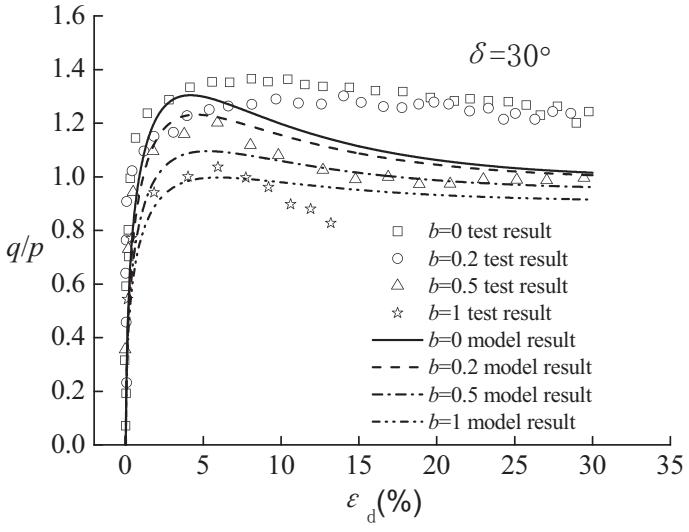

FIGURE 32 Comparison between test data and prediction of relationship between stress ratio and deviatoric strain for Leighton Buzzard sand under $\delta = 30°$

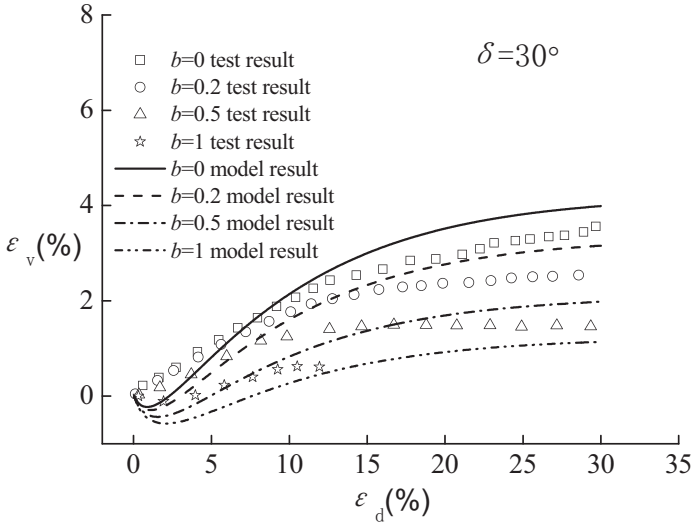

FIGURE 33 Comparison between test data and prediction of volume strain and deviatoric strain relationship for Leighton Buzzard sand under $\delta = 30°$

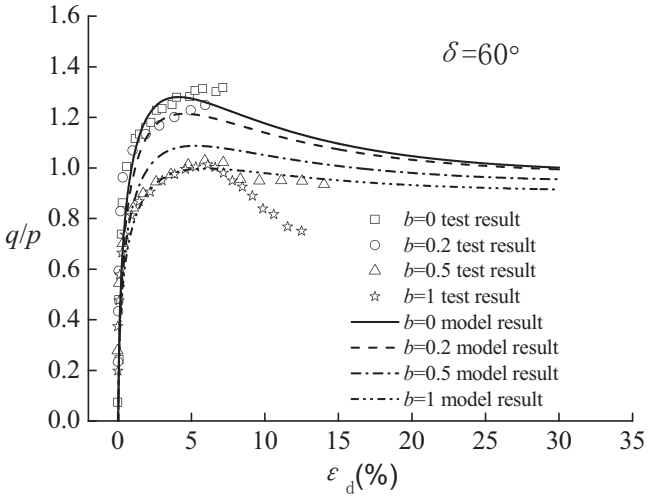

FIGURE 34 Comparison between test data and prediction of stress ratio and deviatoric strain relationship for Leighton Buzzard sand under $\delta = 60°$

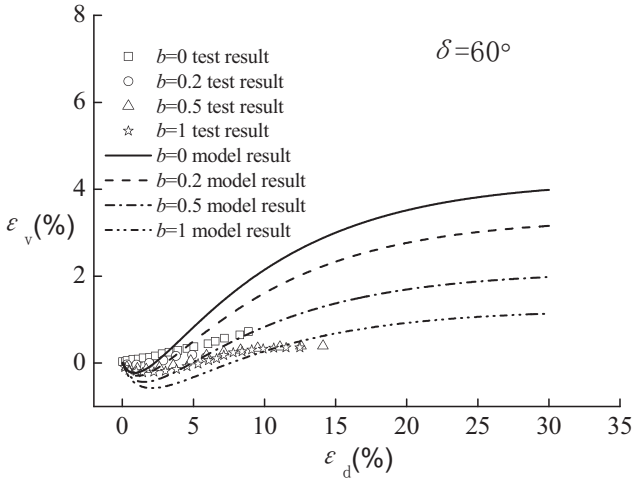

FIGURE 35 Comparison of results from test data and prediction of volume strain and deviatoric strain relationship for Leighton Buzzard sand under $\delta = 60°$

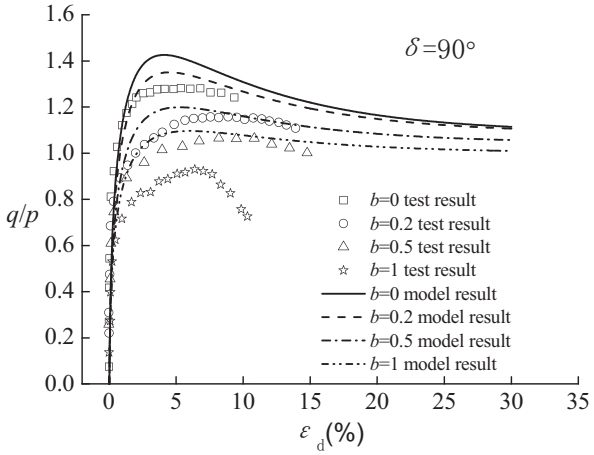

FIGURE 36 Comparison between test data and prediction of stress ratio and deviatoric strain relationship for Leighton Buzzard sand under $\delta = 90°$

Lode angle conducted by Yang.[45] The continuous curves represent predicted results from the DUH model modified by the proposed transformation stress method. The angle between the major principal stress and the normal direction of the sedimentary surface which equals 0°, 30°, 60°, and 90° are defined as the initial loading conditions, and the stress-strain relationship curves under the b values of 0, 0.2, 0.5, and 1 are investigated to indicate the effect of the original anisotropy.

Figure 30 shows the tested and predicted results when the major principal stress is perpendicular to the loading direction of the sedimentary plane. The relationship between the stress ratio and the deviatoric strain is clear, therefore, the modified model can indicate the decreases of stress ratio strength and the strain-softening phenomenon induced by the increase of b reasonably. Figure 30 shows the comparison between the volume strain and the deviatoric strain. The dilatational volume strain gradually decreases with the increase in the value of b, which represents that the model is capable to indicate the above characteristics.

Figures 31 and 32 present the comparison of the stress-strain relationship when $\delta = 30°$. To indicate the decrease of the stress ratio with the increase in the value of b, the peak stress of the curve decreases with the increase of δ compared with the $b = 0°$ loading condition. The model can indicate the above law after the modification by the proposed transformation stress method reasonably. The volume strain properties in Figure 32 can also be described appropriately by the model.

Figures 34 and 35 present the comparison of the stress-strain relationship when $\delta = 60°$. According to Figure 34, with the increase of δ, the stress ratio of each curve decreases slightly. This phenomenon can be indicated by the modified model. According to Figure 35, the dilatancy of the volumetric strain is less than that when $\delta = 30°$, this feature has also been indicated by the modified model.

Figures 36 and 37 present the comparison of the stress-strain relationship when $\delta = 90°$. The tested results indicate that the peak stress ratio of each curve decreases slightly, but the stress ratio strength predicted by the modified model is excessively high. According to Figure 37, the predicted value of shear dilatation is slightly larger than the tested result.

In order to describe the failure features of the proposed strength criterion under the general stress condition, the torsional shear test of hollow cylinder performed on saturated sand by Lade[46] is adopted for prediction. The disposition surface of sand is horizontal, the internal and external radial pressures of sand cylindrical sample is maintained at 202 kPa, and the magnitude and direction of the intermediate principal stress is the same as the radial pressure. The axial stress and tangential stress of the cylinder change with the torsional shear stress, which corresponds to the rotation of the direction of the major and minor principal stresses in the cylinder, this is exactly the rotated loading phenomenon of the principal stress. The angle between the major principal stress and the depositional surface (ζ) is related to the parameter b of the intermediate principal stress. When $-45° < \zeta < 45°$, $b = \sin 2\zeta$; when $-90° < \zeta \leftarrow 45°$ or $45° < \zeta < 90°$, then $b = \cos 2\zeta$.

Figure 38 shows the tested and predicted results of the relationship between the difference of axial stress and tangential stress and shear stress in the cylindrical plane. The comparison indicates that the T-strength criterion with the transversely isotropic concept can also well describe the failure state under general stress state. Figure 39 represents the comparison between tested and predicted results of the relationship between the middle principal stress parameter b and the internal friction angle φ. With the increase of parameter b of the middle principal stress, the internal friction angle increases first and then decreases, this trend has been indicated by the prediction curve which is consistent with the tested result.

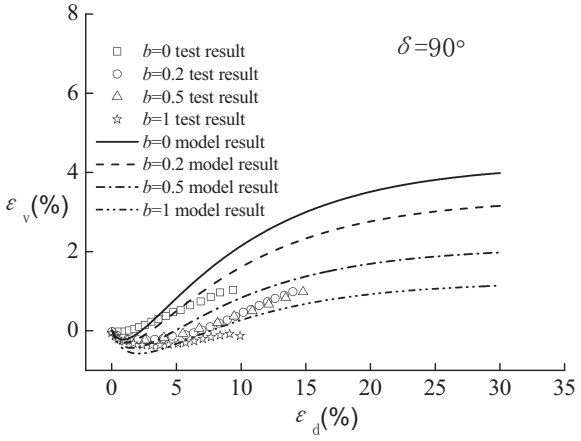

FIGURE 37 Comparison between test data and prediction of volume strain and deviatoric strain relationship for Leighton Buzzard sand under $\delta = 90°$

FIGURE 38 Comparison between test data and prediction of shear stress $\sigma_{z\theta}$ and deviatoric stress (σ_z–σ_θ) for dry-pluviated sand

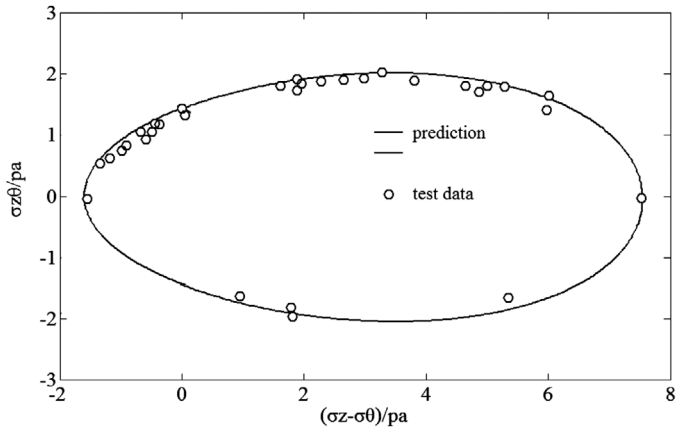

However, when b > 0.3, the predicted result is higher than the tested result. This phenomenon can be mainly attributed to the occurrence of shear band in the tested sample when b > 0.3 and the significant affect from the intermediate principal stress. The phenomenon of the shear band decreases the tested value of the internal friction angle; therefore, the tested value of the internal friction angle is lower than the real value.

5 | MODEL LIMITATIONS

Based on the anisotropic properties of geotechnical materials, this paper summarizes the experimental results of geotechnical materials and indicates the significant effect of macroscopic deposition of geotechnical materials on the final failure stress ratio. The T-strength criterion considers the contribution from cohesion and friction to the failure stress ratio, and indicates that the isotropic geomaterial is a frictional material which behavior is determined by the ratio of the principal shear stress and the normal stress on the effective slip surface. The influence of the DP on the failure stress ratio can be considered as follows: the angle between the effective slip plane and the DP is adopted as the state parameter indicating the transversely isotropic property. The effect of transversal isotropy on the failure stress ratio is based on the following intuitive conjecture: when the effective slip plane and the deposition plane are parallel to each other, the corresponding minimum stress ratio strength value can be determined; when the effective slip plane and the deposition plane are perpendicular to each other, the corresponding maximum stress ratio strength can be obtained. When the angle between the effective slip plane and the deposition plane is determined, the corresponding stress ratio strength will be between the maximum and minimum stress ratio strengths. Based on the above ideas, the T-strength criterion formula which can take the transversely isotropic properties into account is established. Moreover, the transformation stress formula is developed based on the transformation stress method. The constitutive model expressed by the two-dimensional stress variables,

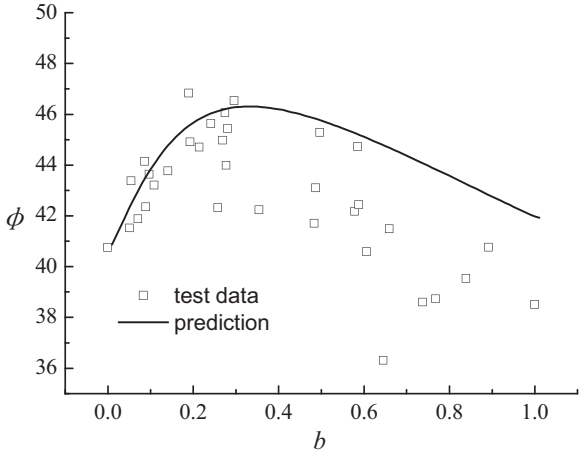

FIGURE 39 Comparison between test data and prediction of relationship between friction angle φ and intermediate principal stress ratio b for dry-pluviated sand

p and q, can be conveniently extended to the three-dimensional constitutive model. The above formula is based on the rule of experimental results and reasonable conception. In addition, the effectiveness of the above transversely isotropic criterion and its transformed stress method have been verified by experiment results, indicating that it can be used to describe the failure characteristics of geomaterials and indicate the effect of the transversely isotropic property on the stress-strain relationship. Moreover, as the T-strength criterion can be used to describe the damage curves from the von Mises criterion to the SMP criterion on the deviatoric plane, the proposed transverse isotropic T-strength criterion can also be used to describe the damage characteristics of metals, rocks, concrete, sand, and other materials. The transversely isotropic property not only has a significant influence on the failure properties of geotechnical materials, but also has a considerable effect on the deformation properties of geotechnical materials. The transversely isotropic properties also have great effects on the law of shear shrinkage and the dilatation of geotechnical materials.

Meanwhile, the transversely isotropic property has a significant effect on the increase or the decrease of the shear modulus of geotechnical materials. For example, when the major principal stress is perpendicular to the deposition plane, the shear modulus under the triaxial compression path is greater than that when the major principal stress is parallel to the deposition plane. Nevertheless, different angles between the major stress and the deposition surface will lead to different phase transformation stress ratios. In addition, the angle between the major principal stress and the deposition surface also results in completely different final volumetric strain values. However, the three-dimensional method proposed in this paper only deals with the stress based on strength criterion, and the effect of the transversely isotropic property of this constitutive model on the deformation properties is not considered adequately. In order to provide a reasonable approach to the model, the influence of transverse isotropy on the deformation properties of rock and soil materials should be analyzed, the state parameters that indicate the transverse isotropy should also be considered in the dilatancy equation and the hardening parameters of the constitutive models. These limitations also indicate the direction for further study and necessary improvement of the mentioned model.

6 | CONCLUSIONS

To demonstrate the influence of the sedimentary plane on the strength characteristics of geotechnical materials, the inclined angle between the effective slip plane and the sedimentary plane is introduced as a state parameter indicating the transversely isotropic properties to the proposed T-strength criterion, and the inclined angle was adopted to construct the slant plane stress strength ratio formula to demonstrate the effect of transversely anisotropic characteristics. Combined with the strength formula of the power function on the meridional plane, the general strength expression indicating the transverse isotropy of geotechnical materials is obtained. Based on the idea that transforming the anisotropic factors first and then the influencing factors of the principal stress, the stress transformation formula indicating the transverse isotropy was developed. This equation describes the transformation process from the general transverse anisotropic stress space to the isotropic stress space. The following conclusions and findings can be deduced:

(1) Based on the existing formula of the T-criterion, the original T-criterion is generalized to the strength criterion that can consider the transversely isotropic property by adding one parameter, and the parameters are easily determined by traditional tests with clear physical meaning.
(2) The proposed anisotropic strength formula is not only applicable to geotechnical materials, but also applicable to metal, rock, concrete, and other materials with a certain cohesion. All these materials have certain primary anisotropic properties.
(3) The proposed transverse stress equation can easily extend the existing two-dimensional model to the general stress-strain model which considers the effect of transverse isotropy.

ACKNOWLEDGEMENTS

This study was supported by the National Natural Science Foundation of China for young scholars (Grant No. 11402260), National Natural Science Foundation of China (Grant No. 42177170), and Natural Science Foundation of Hebei Province in China (Grant No. E2021508031).

DATA AVAILABILITY STATEMENT

All data, models, and code generated or used during the study appear in the submitted article.

ORCID

Zheng Wan https://orcid.org/0000-0002-0687-4935

REFERENCES

1. Oda M. Initial fabrics and their relations to mechanical properties of granular materials. *Soils Found*. 1972;12(1):17–36.
2. Duncan JM, Seed HB. Strength variation along failure surfaces in clay. *J Geotech Eng Div ASCE*. 1966;92(SM6):81–104.
3. Abelev A, Lade PV. Characterization of failure in cross-anisotropic soils. *J Eng Mech ASCE*. 2004;130(5):599–606.
4. Abelev AV, Lade PV. Effects of cross-anisotropy on three-dimensional behavior of sand. I: stress-strain behavior and shear banding. *J Eng Mech ASCE*. 2003;129(2):160–166.
5. Kirkgard MM, Lade PV. Anisotropy of normally consolidated San Francisco Bay Mud. *Geotech Test J ASTM*. 1991;14(3):231–246.
6. Kirkgard MM, Lade PV. Anisotropic three-dimensional behavior of a normally consolidated Clay. *Can Geotech J*. 1993;30(4):848–858.
7. Yong RN, Silvestri V. Anisotropic behaviour of a sensitive clay. *Can Geotech J*. 1979;16:335–350.
8. Nishimura S, Minh NA, Jardine RJ. Shear strength anisotropy of natural London clay. *Géotechnique*. 2007;57(1):49–62.
9. Yamada Y, Ishihara K. Anisotropic deformation characteristics of sand under three-dimensional stress conditions. *Soils Found*. 1979;19(2):79–94.
10. Ochiai H, Lade PV. Three-dimensional behavior of sand with anisotropic fabric. *J Geotech Eng*. 1983;109(10):1313–1328.
11. Miura S, Toki S. Anisotropy in mechanical properties and its simulation of sands sampled from natural deposits. *Soils Found*. 1984;24(3):69–84.
12. Hight DW, Gens A, Symes MJ. The development of a new hollow cylinder appratus for investigating the effects of principal stress rotation in soils. *Géotechnique*. 1983;33(4):355–383.
13. Tatsuoka F, Nakamura S, Huang CC, Tani K. Strength anisotropy and shear band direction in plane strain tests of sand. *Soils Found*. 1990;30(1):35–54.
14. Pradhan TBS, Tatsuoka F, Horii N. Simple shear testing on sand in a torsional shear apparatus. *Soils Found*. 1988;28(2):95–112.
15. Oda M, Nakayama H. Yield function for soil with anisotropic fabric. *J Eng Mech ASCE*. 1989;115(1):89–104.
16. Li XS, Dafalias YF. Constitutive modeling of inherently anisotropic sand behavior. *J Geotech Geoenvir Eng ASCE*. 2002;128(10):868–880.
17. Dafalias YF, Taiebat M. Rotational hardening with and without anisotropic fabric at critical state. *Géotechnique*. 2014;57(1):49–62.
18. Pietruszczak S, Lydzba D, Shao JF. Modelling of inherent anisotropy in sedimentary rocks. *Int J Solids Struct*. 2002;39:637–648.
19. Mroz Z, Maciejewski J. Failure criteria of anisotropically damaged materials based on the critical plane concept. *Int J Numer Anal Meth Geomech*. 2002;26:407–431.
20. Hashiguchi K, Ozaki S, Okayasu T. Unconventional friction theory based on the subloading surface concept. *Int J Solids Struct*. 2005;42:1705–1727.
21. Zhang L-W, Zhang J-M, Zhang G. SMP-based anisotropic strength criteria of granular materials. *Chin J Rock Mech Eng*. 2008;30(8):1107–1111. in Chinese.
22. Wei Cao, Rui Wang, Zhang Jian-min. New strength criterion for sand with cross-anisotropy. *Chin J Rock Mech Eng.* 2016;38(11):2026-2032. in Chinese.
23. Yao Y-P, Kong Y-X. Research on the cross-anisotropic soils strength and failure criterion. *J Hydraul Eng*. 2012;43(1):43-50. in Chinese.
24. Kong YX, Zhao JD, Yao YP. A failure criterion for cross-anisotropic soils considering microstructure. *Acta Geotech*. 2013;8(6):665-673.
25. Lu D, Liang J, Wang G, Du X. Three-dimensional strength criterion for transverse isotropic geomaterials. *Chin J Geotech Eng.* 2018;40(1):54-63. in Chinese.

26. Yang Liu. Anisotropic strength criteria of sand: inherent anisotropy. *Chin J Geotech Eng.* 2013;35(8):1526-1534. in Chinese.
27. Li X-F, Huang M-S, Qian J-G. Failure criterion of anisotropic sand with method of macro-meso incorporation. *Chin J Rock Mec Eng.* 2010;29(9):1885-1892. in Chinese.
28. Gao ZW, Zhao JD. Efficient approach to characterize strength anisotropy in soils. *J Eng Mech*. 2012;138(12):1447-1456.
29. Gao ZW, Zhao JD, Yao YP. A generalized anisotropic failure criterion for geomaterials. *Int J Solids Struct*. 2010;47(22-23):3166-3185.
30. Maosong H, Xuefeng L, Jiangu Q. Strain localization of Anisotropic sand. *Chin J Rock Mech Eng.* 2012;34(10):1772-1780. in Chinese.
31. Wang GS, Lu DC, Du X, Li M, Chin J. Dynamic multiaxial strength criterion for concrete developed based on the S criterion. *Chin J Theor Appl Mech.* 2016;48(3):636–653. in Chinese.
32. Gao J, Yang H, Jiang Y, et al. Study of three-shear stress unified strength theory. *Chin J Theor Appl Mech.* 2017;49(6):1322-1334. in Chinese.
33. Wan Z, Guo J, Jinxue Guo. A kind of strength and yield criterion for geomaterials and its transformation stress method. *Chin J Theor Appl Mech.* 2017;49(3):726–740. in Chinese.
34. Wan Z, Yao Y, Meng D. An elastoplastic constitutive model of concrete under complicated load. *Chin J Theor Appl Mech.* 2016;48(5):1159-1171. in Chinese.
35. Matsuoka H, Jun-Ichi H, Kiyoshi H. Deformation and failure of anisotropic and deposits. *Soil Mech Found Eng*. 1984;32(11):31–36. in Japanese.
36. Guo ZH, Guo YT, Xu Y, Ye XG, Li WZ. Nonlinear elastic orthotropic constitutive model for concrete. *J OF Tsinghua University (Science and Technology)*. 1997;37(6):78-81.
37. Yao YP, Zhou AN, Lu DC. extended transformed stress space for geomaterials and its application. *J Eng Mech ASCE*. 2007;133(10):1115–1123.
38. Yao YP, Sun DA, Matsuoka H. A unified constitutive model for both clay and sand with hardening parameter independent on stress path. *Comput Geotech*. 2008;35(2):210–222.
39. Yao YP, Yamamoto H, Wang ND. Constitutive model considering sand crushing. *Soils Found*. 2008;48(4):603–608.
40. Matsuoka H, Yao YP, Sun DA. The cam-clay models revised by the smp criterion. *Soils and Foundation*. 1999;39(1):81–95.
41. Niandou H, Shao JF, Henry JP, et al. Laboratory investigation of the behaviour of Tournemire shale. *Int J Rock Mech Min Sci*. 1997;34(1):3—16.
42. Banerjee PK, Yousif NB. A plasticity model for the mechanical behavior of anisotropically consolidated clay. *Int J Numer Anal Methods Geomech*. 1986;10:521–541.
43. Wan Z. A cyclic UH model for sand. *Earthq Eng Eng Vib.* 2015;14(2):229–238.
44. Rowe P. The stress-dilatancy relation for static equilibrium of an assembly of particles in contact. *Proc R Soc Lond*. 1962;269:500-527.
45. Yang LT, Li X, Yu HS, Wanatowski D. A laboratory study of anisotropic geomaterials incorporating recent micromechanical understanding. *Acta Geotech*. 2016;11(9):1111-1129.
46. Lade PV, Nam J, Hong WP. Shear banding and cross-anisotropic behavior observed in laboratory sand tests with stress rotation. *Can Geotech J*. 2008;45:74-84.

How to cite this article: Wan Z, Liu Y, Cao W, Wang Y, Xie L, Fang Y. One kind of transverse isotropic strength criterion and the transformation stress space. *Int J Numer Anal Methods Geomech*. 2021; 1–40. https://doi.org/10.1002/nag.3322

APPENDIX A: THE DEDUCTION OF T CRITERION

In the general conventional triaxial compression loading test, the failure mode of the tested sample is shown in Figure A1.

As shown in Figure A1, under a pair of loading stresses of $\sigma 1$, $\sigma 3$ in the triaxial compression test, the angle between the sliding plane and the loading plane of $\sigma 1$ is $45°+\varphi e13/2$. Here, $\varphi e13$ is the equivalent friction angle corresponding to the tangent contact point of the power function strength line and the Mohr circle.

In the two-dimensional plane coordinate σ-τ system, the assumed strength line is a general linear line representing the Mohr-Coulomb model with consideration of cohesion. The line can be expressed as:

$$\tau_1 = k\sigma + b \tag{A1}$$

when $b = 0$, the above expression is transferred to a straight line passing through the origin point, which is written as below and represents the Mohr-Coulomb criterion without cohesion:

$$\tau_1 = k\sigma \tag{A2}$$

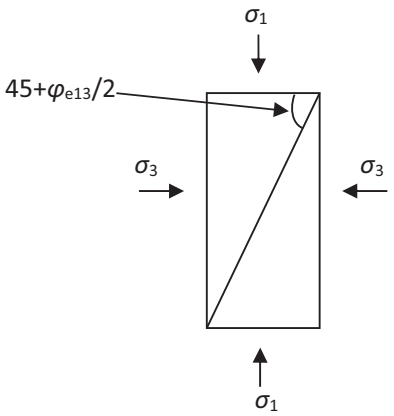

FIGURE A1 The slip plane in a sample for triaxial test

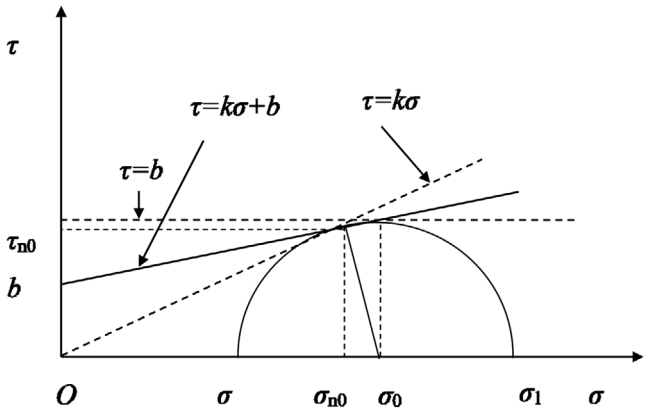

FIGURE A2 The circumscribed figure between the strength line and mohr's circle

When $k = 0$, then the line degrades to a horizontal line as below:

$$\tau_1 = b \tag{A3}$$

When $k > 0$, then the expression represents a general straight line.

For any value greater than zero, it is assumed that the sample fails when the straight line is tangent to the Mohr circle and this tangent contact point represents the failure state, as illustrated in Figure A2.

As shown in Figure A1, when the line is tangential with the Mohr circle, the tangent contact point is p(σn0,τn0). The strength line is expressed as $\tau 1 = k\sigma + b$, and the function of Mohr circle is expressed as $\tau 2 = (R2-(\sigma-\sigma 0)2)0.5$. Here, R represents the radius of the Mohr circle, and $\sigma 0$ represents the abscissa value of the center of the Mohr circle.

As shown in Figure A1, the effective sliding angle can be expressed with the external tangential line of the Mohr circle. When the line passes through the original point, it corresponds to the maximum value of the effective internal friction angle that can be expressed as below:

$$\tan \varphi_e = \frac{R}{\sqrt{\sigma_0^2 - R^2}} \tag{A4}$$

When the tangential line is parallel to the abscissa, the corresponding effective internal friction angle is the smallest and equal to zero. It is obvious that the line representing a general effective internal friction angle is between the above two lines, and the general effective friction angle can be expressed by interpolating a parameter t. The parameter t is set

to represent the weight distribution of friction and cohesion, and its value is between 0 and 1.

$$\tan\varphi_e = \frac{tR}{\sqrt{\sigma_0^2 - R^2}} \quad 0 \le t \le 1 \tag{A5}$$

Obviously, when $t = 0$, tanφe = 0; when $t = 1$, then the effective friction angle satisfies the following equation:

$$\tan\varphi_e = \frac{R}{\sqrt{\sigma_0^2 - R^2}} = \frac{(\sigma_1 - \sigma_3)}{2\sqrt{\sigma_1\sigma_3}} \tag{A6}$$

Similar to the concept of the SMP space sliding plane, there is also an effective sliding plane in three-dimension physical space. The stresses acting on the sliding plane are the equivalent shear stress τen and equivalent normal stress σen, which can be deduced as below:

$$L_{EB} = \tan\varphi_{e13} + \sec\varphi_{e13} \tag{A7}$$

$$L_{EC} = \tan\varphi_{e23} + \sec\varphi_{e23} \tag{A8}$$

$$\tan\varphi_{e13} = \frac{tR}{\sqrt{\sigma_0^2 - R^2}} = \frac{t(\sigma_1 - \sigma_3)}{2\sqrt{\sigma_1\sigma_3}} \tag{A9}$$

$$\tan\varphi_{e23} = \frac{tR}{\sqrt{\sigma_0^2 - R^2}} = \frac{t(\sigma_2 - \sigma_3)}{2\sqrt{\sigma_2\sigma_3}} \tag{A10}$$

The parameter t is introduced to represent the proportional weight of friction and cohesion. The corresponding effective friction angle can be expressed as the arctangent value of the tangential line of the Mohr circle. The corresponding line intercept can be expressed as:

$$L_{EB} = \frac{t(\sigma_1 - \sigma_3) + \sqrt{t^2\left(\sigma_1^2 + \sigma_3^2\right) + (4 - 2t^2)\sigma_1\sigma_3}}{2\sqrt{\sigma_1\sigma_3}} \tag{A11}$$

$$L_{EC} = \frac{t(\sigma_2 - \sigma_3) + \sqrt{t^2\left(\sigma_2^2 + \sigma_3^2\right) + (4 - 2t^2)\sigma_2\sigma_3}}{2\sqrt{\sigma_2\sigma_3}} \tag{A12}$$

As shown in Figure A3, the angles ∠ABE and ∠ACE can be completely determined, and given the hypothesis of the spatial sliding plane is true, the angle ∠CBE can be calculated from the tangent value of the trigonometric function.

$$\tan\left(45^\circ - \varphi_{e12}/2\right) = \frac{L_{EC}}{L_{EB}} \tag{A13}$$

It can be obtained that

$$\varphi_{e12} = 2\arctan\left(\frac{L_{EB} - L_{EC}}{L_{EB} + L_{EC}}\right) \tag{A14}$$

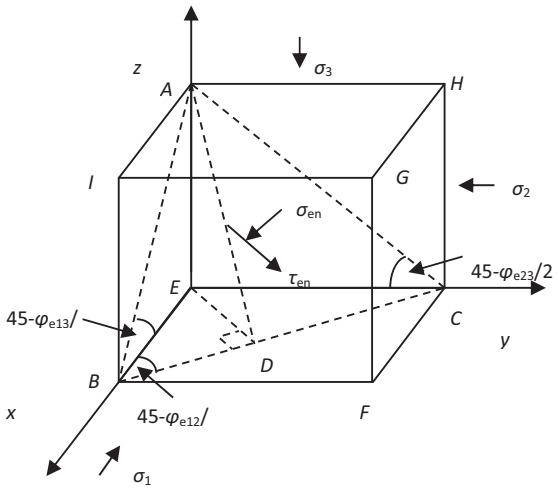

FIGURE A3 The slip plane in three-dimensional space coordinate

Substituting (A7) and (A8) into (A14):

$$\varphi_{e12} = 2\arctan\left(\frac{\tan\varphi_{e13} - \tan\varphi_{e23} + \sec\varphi_{e13} - \sec\varphi_{e23}}{\tan\varphi_{e13} + \tan\varphi_{e23} + \sec\varphi_{e13} + \sec\varphi_{e23}}\right) \tag{A15}$$

Equation (A15) is the relationship between the three angles indicating the spatial location of the effective sliding plane (ESMP).

The directional cosine of the spatial sliding plane can be expressed as ω1(l1, m1, n1). For geomaterials, there is a spatial deposition surface (DP) in the spatial coordinate system, and the directional cosine of the deposition plane can be expressed as ω2(l2, m2, n2). Thus, the angle between the above two spatial planes can be expressed by the arccosine value of the dot production of two normal vectors of the two planes.

$$\alpha = \arccos\left(\frac{l_1 l_2 + m_1 m_2 + n_1 n_2}{\sqrt{l_1^2 + m_1^2 + n_1^2}\sqrt{l_2^2 + m_2^2 + n_2^2}}\right) \tag{A16}$$

The failure of the element can be expressed by the stress ratio index. The stress ratio changes with the above angle α. Obviously, when $\alpha = \alpha\min = 0°$, the spatial sliding plane coincides with the spatial deposition plane. At this time, the connection between the deposition layers is the weakest, therefore the strength is the lowest. When $\alpha = \alpha\max$, the angle between the spatial sliding plane and the spatial deposition plane reaches the largest value, and it is most difficult to destroy the material, therefore the strength is the largest. When $0° < \alpha < \alpha\max$, the stress ratio is between the above values, and can be expressed by nonlinear interpolation function according to the monotonic changing relationship between the strength and the value of α.

$$M_\alpha = f\left(M_{\min}, M_{\max}, \alpha\right) \tag{A17}$$

According to the relationship of angles illustrated in Figure A3, the normal direction of the spatial disposition plane can be expressed as:

$$\omega 2\,(\mathrm{l2}, \mathrm{m2}, \mathrm{n2}) = \omega 2\,(\cos\alpha 1\cos\alpha 2,\ \cos\alpha 1\sin\alpha 2,\ \sin\alpha 1) \tag{A18}$$

Firstly, the ratio of principal shear stress to the principal normal stress expressed by principal stresses of the spatial sliding plane is calculated.

$$r = \sqrt{L_{EB}^2 + L_{EC}^2 + L_{EB}^2 L_{EC}^2} \tag{A19}$$

The component of normal vector of the effective spatial sliding plane can be expressed as:

$$l_1 = \frac{L_{EC}}{r} \tag{A20}$$

$$m_1 = \frac{L_{EB}}{r} \tag{A21}$$

$$n_1 = \frac{L_{EB}L_{EC}}{r} \tag{A22}$$

$$s_{\Delta AEB} = \frac{L_{EB}}{2} \tag{A23}$$

$$s_{\Delta AEC} = \frac{L_{EC}}{2} \tag{A24}$$

$$s_{\Delta EBC} = \frac{L_{EB}L_{EC}}{2} \tag{A25}$$

$$\sin \angle BAC = \frac{r}{\sqrt{1+r^2}} \tag{A26}$$

Based on the relationship of trigonometric function, it is clear that:

$$\tan \angle BAC = r \tag{A27}$$

As shown in Figure A3, the equivalent normal stress can be determined from the force balance relationship of the regular tetrahedron.

The equivalent normal stress can be expressed as:

$$\sigma_{en} = \frac{l\sigma_1 s_{\Delta AEC} + m\sigma_2 s_{\Delta AEB} + n\sigma_3 s_{\Delta EBC}}{s_{\Delta BAC}} \tag{A28}$$

$$\sigma_{en} = \frac{\sigma_1 EC^2 + \sigma_2 EB^2 + \sigma_3 EB^2 EC^2}{r^2} \tag{A29}$$

$$\tau_{en} = \sqrt{\left(\frac{\sigma_1 L_{EC}}{r}\right)^2 + \left(\frac{\sigma_2 L_{EB}}{r}\right)^2 + \left(\frac{\sigma_3 L_{EB}L_{EC}}{r}\right)^2 - \sigma_{en}^2} \tag{A30}$$

The ratio of the principal shear stress to the principal normal stress on the effective sliding plane is:

$$\frac{\tau_{en}}{\sigma_{en}} = \tan \varphi_{mo} = \frac{L_{EB}L_{EC}\sqrt{(\sigma_1-\sigma_2)^2 + L_{EB}^2(\sigma_2-\sigma_3)^2 + L_{EC}^2(\sigma_3-\sigma_1)^2}}{\sigma_1 L_{EC}^2 + \sigma_2 L_{EB}^2 + \sigma_3 L_{EB}^2 L_{EC}^2} \tag{A31}$$

where φmo represents the internal friction angle of the effective spatial sliding plane.

Under the triaxial compression condition, Equation (A31) can be expressed as:

$$\frac{\tau_{en}}{\sigma_{en}} = c_1 \tag{A32}$$

The principal stresses can be expressed as:

$$\begin{cases} \sigma_1 = p + \frac{2}{3}q_c \\ \sigma_2 = \sigma_3 = p - \frac{1}{3}q_c \end{cases} \tag{A33}$$

Substituting Equation (A33) into Equation (A31), the function of p, qc can be determined:

$$f(p, q_c) = \frac{q_c L_{EB_c} L_{EC_c} \sqrt{1 + L_{EC_c}^2}}{(p + 2q_c/3) L_{EC_c}^2 + (p - q_c/3) L_{EB_c}^2 \left(1 + L_{EC_c}^2\right)} \tag{A34}$$

$$r_c = \sqrt{L_{EB_c}^2 + L_{EC_c}^2 + L_{EB_c}^2 L_{EC_c}^2} \tag{A35}$$

Adopting the expression method of two-dimensional variables p and q under triaxial compression condition, the stress ratio M = qc/p can be expressed as:

$$L_{EC_c} = 1 \tag{A36}$$

$$L_{EB_c} = \frac{tq_c + \sqrt{t^2\left(2p^2 + 5q_c^2/9 + 2pq_c/3\right) + (4 - 2t^2)\left(p^2 + pq_c/3 - 2q_c^2/9\right)}}{2\sqrt{p^2 + pq_c/3 - 2q_c^2/9}} \tag{A37}$$

where M represents the failure stress ratio corresponding to the triaxial compression path, and Me denotes that corresponding to the triaxial extension path. With the assumption that λ is the ratio of the above stress ratios, then Me = λM.

$$L_{EC_c} = 1 \tag{A38}$$

$$r_c^2 = 2L_{EB_c}^2 + 1 \tag{A39}$$

Equations (A31) and (A34) are the same under the triaxial compression path, therefore the following expressions can be deduced:

$$\frac{3\sqrt{2}q_c L_{EB_c}}{(3p + 2q_c) + 2(3p - q_c) L_{EB_c}^2} = \frac{\sqrt{(\sigma_1 - \sigma_2)^2 + L_{EB}^2(\sigma_2 - \sigma_3)^2 + L_{EC}^2(\sigma_3 - \sigma_1)^2}}{\sigma_1 L_{EC}/L_{EB} + \sigma_2 L_{EB}/L_{EC} + \sigma_3 L_{EB} L_{EC}} \tag{A40}$$

Equation (A40) represents the generalized deviatoric stress strength formula with consideration of isotropy on the deviatoric plane.

Referring to the expression of the GNST criterion[31] on the meridional plane, the power function of average stress with consideration of the hydrostatic pressure effect can be adopted as the strength expression on the meridional plane.

$$q_c = M_f p_r \left(\frac{p + \sigma_0}{p_r}\right)^n \tag{A41}$$

Solving A31, A40, and A41 simultaneously, the final strength expression can be determined:

$$\frac{3p\left(1 + 2L_{EBx}^2\right)\tan\varphi_{mo}}{3\sqrt{2}L_{EBx} - 2\tan\varphi_{mo}\left(1 - L_{EBx}^2\right)} - M_f p_r \left(\frac{p + \sigma_0}{p_r}\right)^n = 0 \tag{A42}$$

Mf can be regarded as a parameter of the stress strength ratio with the consideration of the deposition plane effect and expressed as below:

The effective sliding plane is the failure plane with the consideration of isotropy, while the existence of the deposition plane would affect the final stress strength ratio to a certain extent based on the following two considerations:

The stress strength ratio Mf can be expressed as the function of the angle between the effective sliding plane and the three-dimensional deposition plane. The function needs to satisfy the following conditions:

(1) The relationship between the strength value and the angle between the two planes is monotonic increasing.
(2) It is only related to the angle representing the mutual positions without the consideration for the spatial coordinates to meet the principle of material objectivity.

The internal friction angle of the effective sliding plane is expressed by φmo. In the case of anisotropy, tanφmo is usually not a constant value and can be expressed by tanφmo = F(β, M). β represents the angle between the sliding plane and the spatial deposition plane, and can be regarded as a state parameter indicating the degree of anisotropy. Therefore, the above function contains the information describing the direction and degree of anisotropy.

Similarly, the angle between the effective sliding plane and the spatial deposition plane can be expressed by the arccosine of the dot production of the normal vectors of the two planes as following:

$$\beta = \arccos\left[\frac{L_{EC}\cos\alpha_1\cos\alpha_2 + L_{EB}\cos\alpha_1\sin\alpha_2 + L_{EC}L_{EB}\sin\alpha_1}{r}\right] \tag{A43}$$

Under the triaxial compression path, the simplified Equation (A43) can be expressed as:

$$\beta = \arccos\left[\frac{\cos\alpha_1\cos\alpha_2 + L_{EBc}\cos\alpha_1\sin\alpha_2 + L_{EBc}\sin\alpha_1}{r_c}\right] \tag{A44}$$

It is a common practice to adopt the angle between the maximum principal stress and the deposition plane (δ) as the major parameter assessing the influence of anisotropy on the stress strength ratio. The above methods can partially consider the contribution of anisotropic deposition to the final strength. However, the results of plane strain strength tests on sands conducted by Matsuoka et al.[32] show that the plane strain strength changes in a non-monotonic way with the increasing of δ: the strength decreases first and then increases. When the angle between the spatial sliding plane and the deposition plane (ζ) is adopted to build a relationship, the relationship is monotonic.

By analogy with the monotonic relationship between the angle of the deposition plane and the spatial sliding plane and the stress strength ratio with isotropy characteristic, the case of three-dimensional orthotropic can be further extended. Under this circumstance, the three-dimensional characteristic deposition takes the combined effect of the deposition plane in three directions of principal stresses into account. The characteristic thicknesses of the deposition plane in the three directions of principal stresses are used to determine the characteristic size of each direction. The angle between the characteristic deposition plane and the spatial sliding plane has a monotonic relationship with the final stress strength ratio, which can be simply expressed by the following parabolic function:

$$M_\beta = M_n + (M_x - M_n)\left(\frac{\beta}{\beta_x}\right)^2 \tag{A45}$$

Therefore, the final strength can be expressed as the following:

$$\frac{3p\left(1+2L_{EBx}^2\right)\tan\varphi_{mo}}{3\sqrt{2}L_{EBx} - 2\tan\varphi_{mo}\left(1-L_{EBx}^2\right)} - M_\beta p_r\left(\frac{p+\sigma_0}{p_r}\right)^n = 0 \tag{A46}$$